# Photochemical Degradation and the Global Cycling of Marine Biologically Refractory Dissolved Organic Matter Evaluated with the University of Victoria Earth System Climate Model

## Master Thesis

**Master Program Biological Oceanography**

**GEOMAR-Helmholtz Centre for Ocean Research Kiel**

**July 2016**


**Candidate:** Jiajun Wu
**Supervisors:** Dr. David Keller
Pr. Dr. Andreas Oschlies
**Department:** Marine Biogeochemical Modeling


GEOMAR
Helmholtz-Zentrum für Ozeanforschung Kiel

# Abstract

Ocean is the largest carbon inventory on the earth, which is playing a crucial role in global carbon storage. Variation in oceanic carbon pool will affect atmospheric carbon pool and lead to global climate change. Dissolved organic carbon (DOM) is one of the largest carbon pool in the ocean, of which biologically refractory DOM (RDOM) is a steady and long-time part, which cannot be degraded by biological consumption. Dissolved black carbon (DBC) is also an obvious component of oceanic DOM pool. Photochemical degradation is proved to be an important pathway of RDOM reduction. Recently, several simulations about the life time of RDOM pool and DBC pool were made based on laboratory photochemistry experiments. However, these conclusions were drawn with no consideration of ocean circulations and other important ocean physical processes.

The objective of this thesis was to make a more convincing simulation of RDOM/DBC pool life-time under photochemical degradation. The work was performed using University of Vicroria Earth System Climate Model (Uvic ESCM), a numerical Earth system model of intermediate complexity. Before the experiments, several modifications were made in the model, including increasing the model resolution in the top ocean, addition of Ultraviolet radiation forcing data, addition of RDOM/DBC tracers and building the photochemistry functions. Afterwards, physical evaluations of the modified model were performed.

One experimental part of this thesis was to study the global cycling of RDOM/DBC including the upwelling other physical processes which would influence the photodegradation rate. The initial concentration of RDOM/DBC was set uniformly in the global ocean. After a 6500-yr model running, tracers gathered at equator, tropics/subtropics and other upwelling regions. The Atlantic Ocean finally had most tracer amount among all ocean basins. UVB radiation would penetrate vertically into the water about 30 to 40 meters. UVB radiation and the ocean physical transportation controlled the tracer movement and affected tracer photodegradation.

Another experimental part was to study the global photodegradation of RDOM/DBC. 96.5% of the RDOM pool was degraded by UV radiation in 6500-yr, meanwhile the DBC pool was entirely degraded after 6000-yr. These results varied from the reported predictions (~600-1600 years) according to laboratory experiment results under specified conditions. As the concentration of RDOM/DBC remained stable in the ocean, a hypothesis could be made that there should exist other resources which could balance the pool against photodegradation.

# Introduction

## 1 Marine dissolved organic matter (DOM) & biologically refractory DOM (RDOM)

### 1.1 What is dissolved organic matter (DOM)?

From the beginning of 20th century, people started to focus on the organic component in the seawater. One of the first studies was titled, “Comparison of amount of then matter that is dissolved in the ocean with that present in organisms shows how extraordinarily small the amount of formed mass is compared to that which is unformed” (Pütter, 1907; English translation cited from Dittmar & Stubbins, 2014). Since then it is commonly realized that seawater is composed not only of water (96.5%) and inorganic solutes (3.5%), but also of organic matter (~1.0%), which looks like “nutrient soup”.

Several early unsuccessful early attempts to quantify the dissolved organic contents of seawater were carried out (Pütter, 1909; Raben, 1910;Krogh & Keys, 1934). In the mid-20th century, glass fiber or silver filters had minimal pore sizes of ~0.45-1.0 μm and became the basis of the operational definition that dissolved matters pass such filters (D. Hansell, Carlson, Repeta, & Schlitzer, 2009). Today DOM is operationally defined as the organic constituents of water that have neutral buoyancy and pass through a filter of 0.2–1.0 μm pore size(Dittmar & Stubbins, 2014; Ogawa & Tanoue, 2003; Nebbioso & Piccolo, 2013). Contrarily, those organic contents left on the filter are called particular organic matters (POM). Actually, this is only an arbitrary definition. In reality, POM and DOM are difficult to separate due to no clear difference and a lot of matter, e.g. gels, which are difficult to classify as POM or DOM.

Broadly speaking, DOM mainly contains carbon, hydrogen, oxygen, nitrogen, phosphorous and sulfur. The usual currency for quantifying the DOM has been carbon (Sharp, 2002). A general concept in the past century, which is not commonly used today, was that half weight of the total organic matter poor is two times of the total organic carbon (Krogh, 1934). The component of DOM, which is quantified as total organic carbon, is named as dissolved organic carbon (DOC).

Besides DOC, researches focusing ocean organic nitrogen and phosphorous, which are the main nutrient elements for marine ecosystem, are always based on the quantity and quality of another two main subsets of the same DOM: dissolved organic nitrogen (DON) and dissolved organic phosphorous (DOP). Compared to organic carbon, the global pools of organic nitrogen, phosphorus, and other organic elements are not well constrained. The C: N ratio of DOM is relatively constant in the ocean, averaging 13.6 at the sea surface and 14.7 in the deep ocean (Sipler & Bronk, 2015).

## 1.2 Global inventory and distribution

As carbon is a major element of organic matters, DOC measurements are generally applied to determine the abundance and amount of DOM, and it is also easier to measure DOC than DON or DOP. DOC in the sea is the largest ocean reservoir of reduced carbon, holding greater than 200 times the carbon inventory of marine biomass(D. A. Hansell, Carlson, Repeta, & Schlitzer, 2009), approximately as much carbon (~700 x $10^{15}$ gC, Table 1.1) as is available in atmospheric carbon dioxide (~750 x $10^{15}$ gC, Siegenthaler & Sarmiento, 1993). Although the global inventory is large, DOC exists in the open ocean at extremely low concentrations (34~80 μmol $kg^{-1}$, Hansell, Carlson, Repeta, & Schlitzer, 2009).

Table 1.1 Global inventories of DOC differentiated by depth (Hansell, et al., 2009)

| **Depth (m)** | **DOC (Pg C)** |
|---|---|
| 0-200 | 47 |
| 0-1000 | 185 |
| >1000 | 477 |
| Top-bottom | 662 |

Fig. 1.1(D. Hansell et al., 2009) shows the global distribution of ocean DOM at surface (a) and bottom (b). On the upper layer, higher concentration (~68-80 umol $kg^{-1}$) occurs at trophic and subtropics where the higher primary production lays out more DOM. In general, the surface concentrations of DOC changed depending on the latitudinal(Ogawa & Tanoue, 2003), in the order of the Arctic (70–100 μ M) > subtropical (~80 μ M) > tropical (equatorial) and temperate (60–70 μ M) > subarctic and subantarctic (50–60 M) > Antarctic (40–60 μ μ M). And the vertical stratification of the upper water column favors the slow accumulation of organic matter resistant to biological degradation (Hansell, Carlson, Repeta, & Schlitzer, 2009; Carlson, 2002). The Arctic Ocean is enriched in DOC by the input of terrigenous organic matter via high river fluxes to this area (Dittmar & Kattner, 2003).

In deeper layers (Fig. 1.1 b), North Atlantic Deep Water (NADW) has higher concentration (~42 umol $kg^{-1}$) than deep water in India Ocean and Southern Ocean (~39 umol $kg^{-1}$), while the Pacific

Ocean deep water contains the least DOM. One possible reason for the phenomenon is that during the global distribution of bathypelagic water from the North Atlantic into the North Pacific and back to Antarctica (~1000 yr), heterotrophic microbes slowly consume DOC and drop the concentrations from >50 mM in the deep North Atlantic to 34 mM in the oldest water at mid depth in the Pacific (D. Hansell et al., 2009).

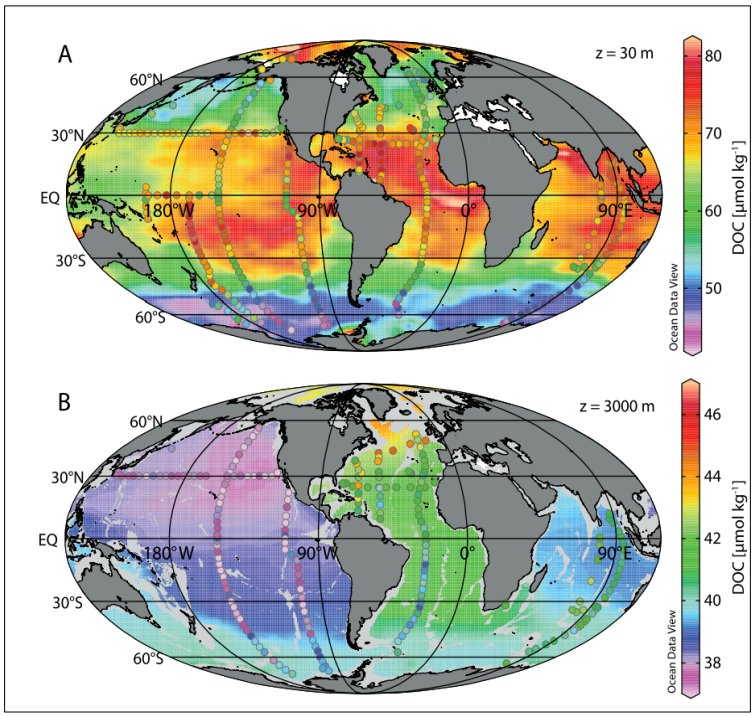


Fig. 1.1 Distributions of dissolved organic carbon (DOC; µmol $kg^{-1}$) at 30 m (A) and 3000 m (B)

## 1.3 Production and sources of DOM

Oceanic DOM is mostly produced by photosynthesis of phytoplankton in the upper layers (~0-200m), as known as the epipelagic zone. Photosynthesizing organisms such as phytoplankton and algae absorbs sunlight in the epipelagic zone and convert inorganic carbon dioxide into organic carbon using the sunlight energy (Fig. 1.2). Marine photosynthesis fixes neatly 10 Pmol-C every year forming organic biomass (Del Giorgio & Williams, 2005; Field, Behrenfeld, & Randerson, 1998). This organic matter is released into the ocean through a number of biological processes (C. a Carlson, 2002):

a. Extracellular release by phytoplankton: Plankton release exopolymeric polysaccharides compounds into water, which will form a loosely associated capsule or sac around them (C. a Carlson, 2002; Gogou & Repeta, 2010; Passow, Alldredge, & Logan, 1994). Specific organic compounds are also released for quorum sensing and other cellular communications (Guan & Kamino, 2001; Nealson & Hastings, 2006; Skindersoe et al., 2008).

b. Grazer mediated release and excretion: Macrozooplankton and microzooplankton remove phytoplankton production and convert the particle organic carbon into dissolved via sloppy feeding (during zooplankton grazing on phytoplankton, pieces of the broken phytoplankton body which cannot be entirely eaten will be released as detritus or DOM), egestion and excretion.

c. Release via cell lysis (both viral and bacterial): viruses produce numerous progeny viruses in the host cell. Then the host cell bursts by the progeny and releases protein, nucleic acid, polymers and etc. into water. Bacteriarially induced lysis of phytoplankton and other bacteria is also observed in experimental cultures. Bacterial lysis is associated with production of external membrane compounds which includes high concentration of cell wall enzyme. The purpose of bacterial lysis is to gain nutrients from lysed cells in order to reducing the competition for existing nutrients.

d. Solubilization of particles: bacteria attached to aggregates can express high levels of hydrolytic ectoenzymes, forming an “enzymatic reactor” which results in the release of DOM.

e. Bacterial transformation and release: heterotrophic bacterioplankton directly release DOM in the form of hydrolytic enzymes and other chemical characteristics in order to capture and digest nutrient molecules in surrounding environment. The release of capsular material is another source of DOM. Bacterioplankton also transform LMW to HMW DOM.

Continentally produced DOM (about 0.02Pmol-C $year^{-1}$) is transported into the ocean through rivers, tidal pumping or aerosols (Dittmar & Stubbins, 2014).

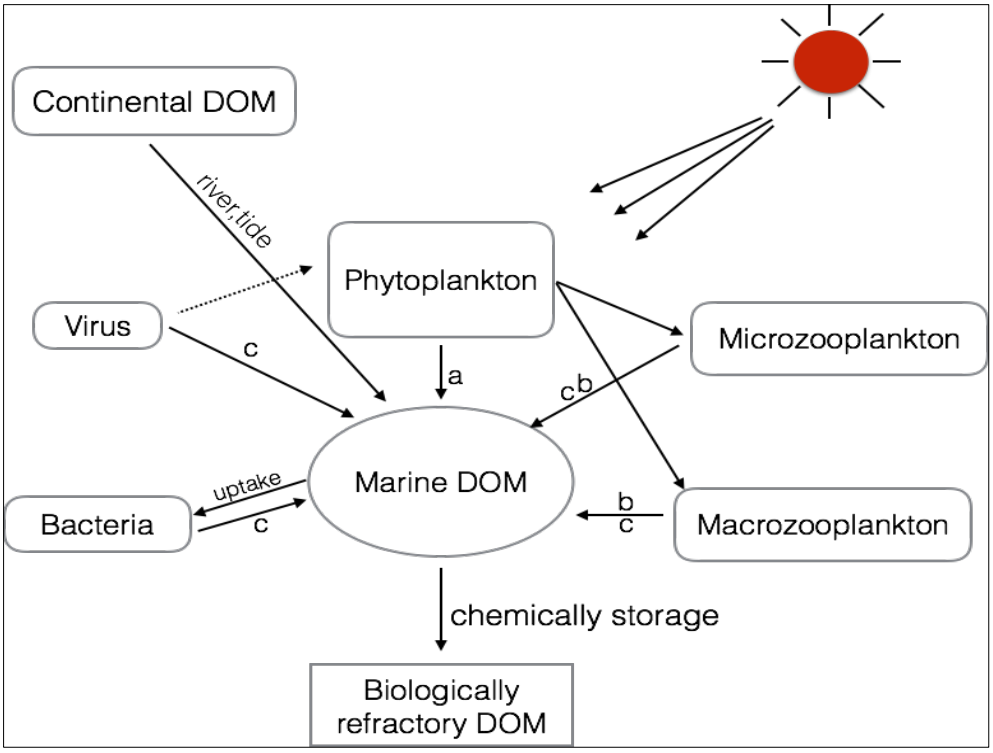


Fig. 1.2 Marine DOM production and sources

## 1.4 Biological utilization of DOM

As mentioned, photosynthesis of phytoplankton mainly take place in the upper layers (~200m). Most of the freshly produced DOM is funneled into "microbial loop". The microbial loop is a general interaction in which DOM is utilized as an energy source, starting with DOM consumed by bacteria via respiration, which makes its way through various trophic levels ultimately to the highest trophic levels. The utilization of this labile DOM represents a large flux of carbon in the ocean. However, with rapid turnover (from minutes to days) it constitutes a very small fraction (~0.01 Pmol-C, < 1%) of the ocean DOC inventory (D. Hansell et al., 2009).

Semilabile DOC is produced mainly in the euphotic zone, holding 15–20% of net community productivity (~ 2 Pg C $yr^{-1}$;D. A. Hansell & Carlson, 1998). Semilabile DOC is not immediately mineralized and instead accumulates in the surface ocean (C. a Carlson, 2002). But semilabile DOC is then rapidly consumed once exported to mesopelagic depths between 100 and 400m (D. A. Hansell, Carlson, & Schlitzer, 2012). The life time of this fraction is from months to years (Craig A. Carlson, Ducklow, & Michaels, 1994)

Though labile DOM is dominant in the epipelagic layer and semilabile DOM obviously decreases from 100m to 400m, biologically refractory DOM (RDOM) is mainly represented in the deep ocean (>1000m) DOC bulk. The RDOM pool is the largest fraction of the bulk dissolved organic

carbon (Williams & Druffel, 1987), holding 52.5 Pmol-C or 650 Gt-C (Dittmar & Paeng, 2009; Dittmar & Stubbins, 2014; Ogawa & Tanoue, 2003). It is dominated by diagenetically altered and low molecular weight (LMW) compounds, which are unavailable to bacteria.

Fig. 1.3 (captured from Figure 4 in Dittmar & Stubbins, 2014) shows the idealized vertical distribution of the DOM pools listed above. Labile DOC is mainly produced and consumed within the epipelagic, semilabile DOC can penetrate into the mesopelagic, and refractory DOC is stable in the bathypelagic on the time scale of deep-ocean mixing. As shown, the RDOM concentration stays invariant from mesopelagic to bathypelagic layers because of the biological resistance of RDOM.

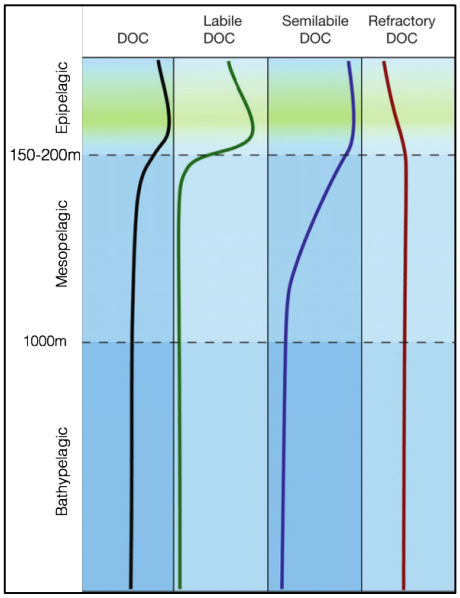


Fig. 1.3 Idealized vertical distribution of marine DOM pools

The apparent average 14C age of RDOM sample from deep ocean water is ~6000 year (Williams & Druffel, 1987), which exceeds the average year of ocean circulation (~1000yr).

Concentration gradients from > 50 μmol $kg^{-1}$ C to ~ 36 μmol $kg^{-1}$ are observed along the water ventilation from the north bottom Atlantic Ocean to the north Pacific deep ocean. As this DOM is biological refractory, there must be degradation pathways, probably abiotic ones, which could possibly explain the great gradients.

## 1.5 Photochemical degradation of RDOM

Two abiotic pathways are reported to be the main removal processes for RDOM: transformation to and/or interaction with suspended particles (Druffel, Williams, Bauer, & Ertel, 1992) and photolysis by ultraviolet (UV) irradiation (Mopper et al., 1991).

As argued above, RDOM has a longer average age than the ocean circulation. Thus, a portion of

RDOM will follow the ocean circulation pathways and be exposed to the sunlight radiation at the ocean surface. Once exposed to surface UV radiation, part of the RDOM will be transformed by photo-oxidation into bio-available LMW (low molecular weight) matters and enter the microbial loop through microbial remineralization (Anderson & Williams, 1999; Benner & Kaiser, 2011; D. Hansell et al., 2009; Mopper et al., 1991). This may also explain why the RDOM in the epipelagic is less than at deeper depths in Fig. 1.3.

UV radiation (UVR) is a significant ecological factor in the marine environment (Häder, Kumar, Smith, & Worrest, 1998). Both UV-B (280–315 nm) and UV-A (315–400 nm) can have important effects on bacterial activities, phytoplankton photosynthesis and photochemical transformations of dissolved organic matter (DOM). There are many pathways for those photochemical reactions. For instance, after absorbing solar radiation, the deactivation of an electronically excited state of DOM molecule occurs via, e.g., ionization of DOM to produce hydrated electrons. These hydrated electrons further react in various ways, such as oxidation (Sulzberger & Durisch-Kaiser, 2009). UVR (mostly UV-B) is also involved in the photochemical degradation of DOM, influencing its bacterial utilization (Mopper & Kieber, 2002).

The attenuation of light in the water column is controlled by two physical processes: scattering and absorption, which depend on the optical properties of seawater. According to the review by Tedetti et.al (2006) the 10% irradiance depth (Z10%, which represents the depth where 10% of surface UVR remains) of UVA and UVB differs among ocean areas. For example, in the Atlantic open ocean, Z10% 305 nm (UVB) and Z10% 340 nm (UVA) can reach 17m and 38m, while for Pacific open ocean they are 8.5m and 25m. On average, the penetration Z10% depth of UVR around the world ocean is 5~35m, which means UVR will be available for the photochemical reactions in the top 40 meters of the ocean.

Through the absorption of solar radiation, RDOM may undergo photochemical reactions using the energy from the absorbed photon, producing many photoproducts which will participate in other reactions and form several products, such as CO and $CO_2$. The absorption of light by DOM initially results in the formation of singlet excited state species ($^1$DOM*) that subsequently decay through a series of photophysical and photochemical pathways, as shown in Fig. 1.4 (Mopper & Kieber, 2002). Studies over the past four decades have demonstrated that marine photochemistry is involved in a variety of chemical reactions of significance to numerous marine, atmospheric and climate-related processes (Mopper & Kieber, 2002).

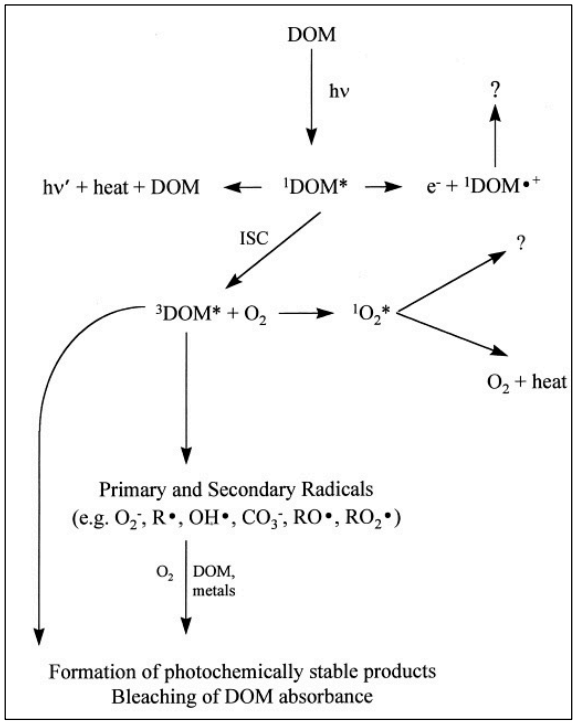


Fig. 1.4 General pathways for the photochemical oxidation of DOM in natural waters

Much research has focused on the photochemical degradation of refractory DOM. Benner et.al (1998) discovered that photo-transformations of deep-water DOM upon exposure to sunlight resulted in enhanced bacterial growth and demonstrated that some refractory components of DOM are rendered bioavailable. Studies have also shown that after a 28-day sunlight irradiation, 95% of dissolved black carbon, one component signature within the DOM pool, could be degraded (Fig. 1.5 from Stubbins, Niggemann, & Dittmar, 2012). That is an obvious decrease, which means that UV light could play an important role in refractory DOM turn over.

Stubbins et al. reported a laboratory work about deep ocean dissolved black carbon photo degradation (DBC, Stubbins, Niggemann, & Dittmar, 2012). DBC is a component signature of deep ocean DOM, which could also count as RDOM. This paper reported the UV degradation rate of DBC and total RDOC (major of deep ocean DOC), which provides us the data for estimating global DBC photochemical turnover. They also estimated that the global DBC inventory lifetime is less than 800 years (28 to 773 years).

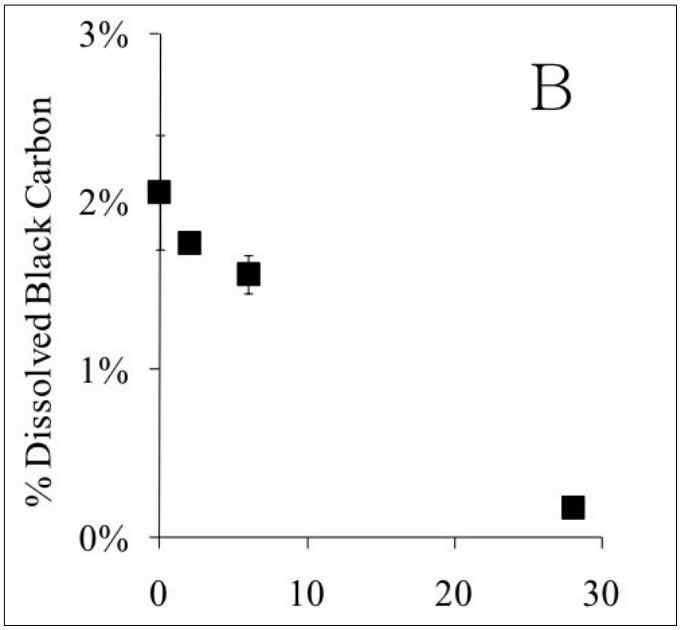


Fig. 1.5 Photodegradation of dissolved black carbon (DBC) in North Atlantic Deep Water over the course of a 28-day irradiation

## 2 Research about DOM photochemistry via numerical models

Numerical models are useful tools for marine biogeochemistry research, covering the estimating scales from global to local and days to millennia. Combining experiment results, observation data and mathematical equations, models are able to estimate biogeochemical processes in the physical, chemical and biological marine environment background. They are also valuable for determining the magnitude and importance of processes that are difficult to measure and observe in the field.

As mentioned above, the global DOM pool is large and still uncharacterized. Some minor changes in the DOM pool could make great effects on global carbon cycling. As for an example, estimated DOC export from the surface ocean represents 20% of total organic carbon flux to the deep ocean, which constitutes a primary control on atmospheric carbon dioxide levels (Hopkinson & Vallino, 2005).

DOC also plays a significant role as a global carbon reservoir. Thus, it is necessary to discover the effect on global marine DOM pool of climate change, such as global warming, ocean acidification, ozone reduction and so on. Investigations with models will be helpful for our understanding of these issues.

Photochemistry of DOM has been an area of increasing interest in recent years. As an important reducing pathway, especially for RDOM, photochemistry is able to convert refractory or semi-refractory DOM into biological labile DOM and fuel microbial loop. Meanwhile, a part of DOM can also be photo degraded into DIC such as CO, which escapes from the ocean via sea-air

gas exchange (Sophia C. Johannessen & Miller, 2001). Although most models lack the full suite of processes(Christian & Anderson, 2002), some studies have been conducted.

Fichot and Miller (2010) proposed a model to calculate depth-resolved marine photochemical fluxes. This model is designed to estimate photochemical rates in the ocean that result solely from the interaction of solar radiation with the dissolved constituents of seawater. Slight variations to the model can be applied to estimate other photochemical processes and also other effects of UV/visible solar radiation on biology and other sensitive systems. For example, this model was updated to parameterize a DOM photochemical degradation rate model for 1086 lakes situated in Sweden (Koehler, Landelius, Weyhenmeyer, Machida, & Tranvik, 2014).

Anderson & Williams (1999) included RDOM in their one dimension model. RDOM here are transferred to labile DOM via photo oxidation. This model suggested that 10% increasing of UV would decrease less than 2% RDOM stock in the ocean over 200 years.

Keller et al. (2011) modified the Anderson & Williams model to explicitly account for photochemical reactions that effect DOM with a rate of 0.004 $\mu$MC (for DOC) or 0.0005 $\mu$MN $d^{-1}$ (for DON). The result showed that photochemical reactions were especially important for turning over the refractory pools of DOM, which converted DOC to DIC at a mean rate of 0.029 $\mu MCd^{-1}$. It was also reported that refractory DOC was degraded into labile DOC at a mean rate of 0.006 $\mu MCd^{-1}$ via photochemical degradation.

Another model from Keller & Hood (2013) contains photochemical reactions as the only pathway for RDOM turnover in estuarine and coastal zones where RDOM is transformed into labile DOM. It was shown in this work that RDOC was converted to labile DOC via photooxidation at rates of 0.23 and 0.68 mmol C $m^{-3}$ $d^{-1}$. The rate of RDON to labile DON was 0.04 and 0.12 mmol N $m^{-3}$ $d^{-1}$. Photochemical reactions were also important for a small amount of DOC converting to DIC.

Although research has shown that UV light does play a key role in marine refractory DOM photochemical degradation, and several mathematical models have been proposed for calculating how the apparent quantum yield (AQY; the ratio of the number of photoproduct molecules formed per photon of light absorbed by the compound responsible for product formation) changes with depth, global estimates of the turn-over time and degradation rates of marine refractory DOM are poorly constrained and mostly based on extrapolations of laboratory turn-over times that do not take into account complexities like ocean circulation.

# 3 Research Questions

In this work, we will add the marine refractory DOM as a new tracer to the ESCM-Uvic to observe the turn-over time of the tracer via photochemical reactions. Key research questions are:

1) How long would it take for an ocean uniformly filled with refractory DOC to turn over with present-day UVR levels at the surface?

2) Where is DOC turnover the highest/lowest and why?

3) What are the factors that control the photochemical turn over rate of refractory DOM

# Methods

## 1 Overview

The current work simulates the photochemical degradation of refractory DOM with the University of Victoria Earth System Climate Model (UVic) version 2.9, in order to find out the global turn-over time of refractory marine DOM. Earth system models (ESMs) integrate the interactions of atmosphere, ocean, land, ice, and biosphere to estimate the state of the climate under a wide variety of conditions. ESMs include physical processes like those in other ocean or climate models but they can also simulate the interaction between the physical climate, the biosphere, and the chemical constituents of the atmosphere and ocean (Heavens et al., 2013). Compared to traditional Climate system models, ESMs always include biogeochemistry. Usually, carbon (C) is most often the key elemental tracer, but other elements, such as nitrogen (N) and phosphate (P) are sometimes included as well.

The current work will mainly be carried out in the 3-D general circulation ocean model (the Modular Ocean Model 2.2; MOM2) component of the Uvic ESCM. This component includes physical parameterizations for diffusive mixing along and across isopycnals, eddy induced tracer advection (Gent and McWilliams, 1990), and a scheme for the computation of tidally induced diapycnal mixing over rough topography (Simmons et al., 2004). An anisotropic viscosity scheme and high Southern Ocean mixing are also included since version 2.9 (Keller et.al, 2012).

The Uvic ESCM model has a spherical grid resolution of 3.6° (zonal) by 1.8° (meridional). The standard model has 19 vertical layers with different thickness, ranging from 50m at the surface to 500m in the deep ocean. Since UVR only penetrates about 10~30m into the upper ocean and thus, is where the photochemical reactions occur, the vertical resolution of the standard model is not suitable for simulating photochemistry. Therefore, the vertical resolution needs to be increased to better simulate photochemical processes (section 3).

Biogeochemical elements are defined as “tracers” inside the model. Tracers are numerical quantities representing some physical mass that are kept track of in each ocean model grid cell as the tracer increases or decreases due to processes like physical transport or biogeochemical reactions.

As a tracer representing refractory DOM has been coded into the Uvic ESCM model, the model will then be modified: the top ocean layer will be divided into thinner ones, aiming at better resolution for UV light and photochemistry processes.

After resolution improvement, an observational dataset of ultraviolet B was added as forcing data

for photochemical processes in the surface. Following that, the UV light and photochemical degradation model component will be added to the model.

The programming language is Fortran 90, and the compiler used here is Intel FORTRAN Composer XE 2013 SP1 for OS X.

Model platform: Mac Pro desk computer from Apple .Inc, which contains 4 memory slots, each of which has a 4GB DDR3 ECC memory, a 3,5 GHz 6-Core Intel Xeon E5 processor. Graphic card is AMD FirePro D500 3072 MB; Thunderbolt display for Mac Pro from Apple .lnc.

Aquamacs was the editor used to code in Fortran 90. The imaging and analysis tool is Ferret (from NOAA's Pacific Marine Environmental Laboratory; http://ferret.pmel.noaa.gov/Ferret/), an interactive computer visualization and analysis environment for analyzing large and complex gridded data sets, and it is widely used to analyze data and create publication quality graphics.

# 2 Refractory DOM tracer addition

The Uvic ESCM is composed of several function code groups, containing common (for common settings), embm (code for atmosphere), ice (code for sea ice and snow), mom (code of MOM2), and etc. The model is forced with several types of data. As mentioned above, a tracer is usually subjected to ocean physical transportation and may participate in chemical and biological processes, representing change of masses or elements. For example, the tracer “oxygen” could participate in biological and physical processes: it can be increased not only by photosynthesis, but also air-sea gas exchange.

The tracer representing RDOM was added by modifying the code in the following files:

- size.h – defines how many tracers are being added. 2 dimensions are added, representing RDOM and RDOM flux.
- UVic_ESCM.f – define the RDOM tracer and any additional parameters associated with it.
- diag.h – define common variables for computing diagnostics .
- diago.F – add variable data for the oceanic diagnostic output.
- mom_tavg.F – add ocean variable data to the main output routine.
- setmom.F – tracers and parameters are initialized here. RDOM initial concentration is set here.

- mw.h – identify the tracers for the memory window.
- npzd.h – add new parameters and rates associated with the new variables here.
- setvbc.F – add surface flux information here.
- timeavgs.h – add model output information that is associated with the new variables here.

The initial concentrations of RDOM are set according to several studies and reports for the experiments (Table. 2.1).

Table. 2.1. RDOM tracer concentration settings

| Item | Concentration [umol-C*Kg$^{-1}$] | References |
|---|---|---|
| Dissolved black carbon (DBC) | 1.05 | Stubbins et al., 2012 |
| RDOM | 50 | Hansell et al., 2009; Anderson & Williams, 1999; Yamanaka & Tajika, 1997 |

# 3 Vertical resolution improvement of Uvic ESCM 2.9

Originally, the ocean is vertically divided into 19 layers in the MOM2 version coupled to the Uvic ESCM 2.9. The Modular Ocean Model (MOM) is a numerical representation of the ocean's hydrostatic primitive equations.

The grid system of MOM2 is composed of T cells and U cells (T stands for tracer, U stands for velocity). Within each T cell is a T grid point, which defines the location of tracer quantities. Similarly, within each U cell is a U grid point defining vertical and meridional velocity components. According to MOM2 notation, $dzt_k$ defines the vertical thickness of a T cell or U cell in centimeters, while $dzw_k$ is the distance between two grid points within neighboring T or U cells. The relationship between $dzw_k$ and $dzt_k$ is shown in Fig. 2.1.

In the current work, a turbulent kinetic energy (TKE) scheme was implemented in UVic ESCM by W. Sijp et al., in order to achieve vertical mixing due to wind and vertical velocity shear (Sijp, Gregory, Tailleux, & Spence, 2012).

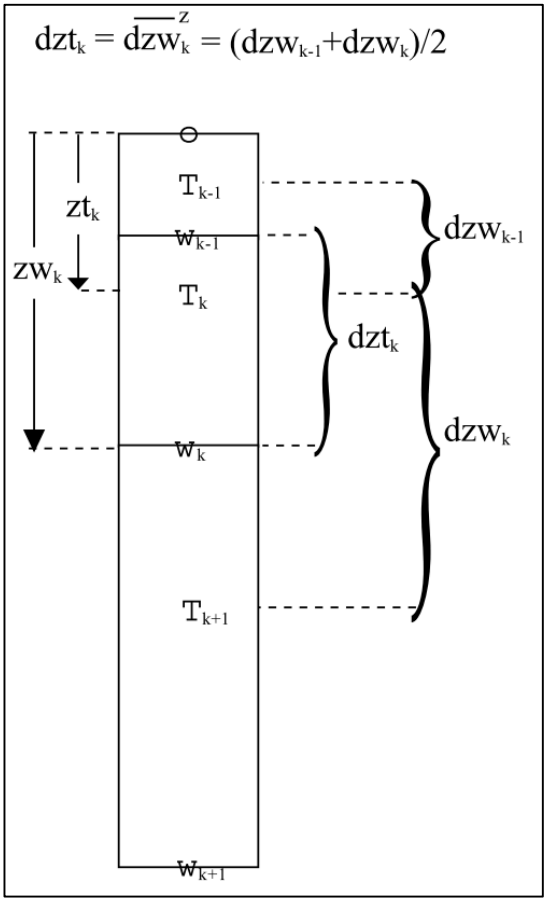


Fig. 2.1 Grid cell construction method in MOM2.

In the standard MOM2 component in UVic the surface layer is 50 meters deep. However, since ultraviolet radiation only penetrates ~ 25 -35m in the ocean surface (Booth & Morrow, 1997; S. C. Johannessen, 2003; Lee et al., 2013; Smith & Baker, 1981) this thickness is less than optimal for simulating photochemical processes. Better simulating photochemical processes thus, requires a higher vertical resolution in the surface ocean.

Therefore, a modification is applied. The first 50 meters are divided into 3 layers with 10m, 20m and 30m ($dzt_k$ value) thicknesses. This modification is calculated via the function in Fig. 2.1, the new vertical solution data is listed in Table. 2.2.

Table 2.2 Modified vertical resolution of MOM2

| Layer | Depth | Depth W | $dzt_k$ | $dzw_k$ |
|---|---|---|---|---|
| 1 | 5 | 10 | 10 | 10 |
| 2 | 15 | 20 | 10 | 10 |
| 3 | 25 | 30 | 30 | 50 |
| 4 | 75 | 130 | 80 | 110 |
| 5 | 185 | 240 | 110 | 110 |
| 6 | 295 | 380 | 140 | 170 |
| 7 | 465 | 550 | 170 | 170 |
| 8 | 635 | 750 | 200 | 230 |
| 9 | 865 | 980 | 230 | 230 |
| 10 | 1095 | 1240 | 260 | 290 |
| 11 | 1385 | 1530 | 290 | 290 |
| 12 | 1675 | 1850 | 320 | 350 |
| 13 | 2025 | 2200 | 350 | 350 |
| 14 | 2375 | 2580 | 380 | 410 |
| 15 | 2785 | 2990 | 410 | 410 |
| 16 | 3195 | 3430 | 440 | 470 |
| 17 | 3665 | 3900 | 470 | 470 |
| 18 | 4135 | 4400 | 500 | 530 |
| 19 | 4665 | 4930 | 530 | 530 |
| 20 | 5195 | 5490 | 560 | 590 |
| 21 | 5785 | 6080 | 590 | 590 |

The Uvic ESCM is forced by several types of data sets in NetCDF (.nc) form, including observation data (i.e. O_sal.nc for salinity, O_temp.nc c for ocean temperature data), basic gridding data (i.e. G_grid.nc for defining T and U cells depths, G_kmt.nc for ocean vertical depth grid level). Uvic uses these datasets once at the beginning of run to set the initial geology, oceanography, atmosphere physic and other conditions for the model run. Meanwhile, some data are used interactively during the simulation, such as A_wind.nc for wind forcing data.

Several MATLAB scripts were created to make new G_grid.nc and G_kmt.nc datasets containing higher vertical resolution settings for Uvic ESCM.

Fig 2.2 compares the grid distribution of modified model with the original one. The total vertical depth at each ocean coordinate is exactly identical, which means that the overall bathymetry of both models is the same while the number of levels in the left subplot have been increased to 21.

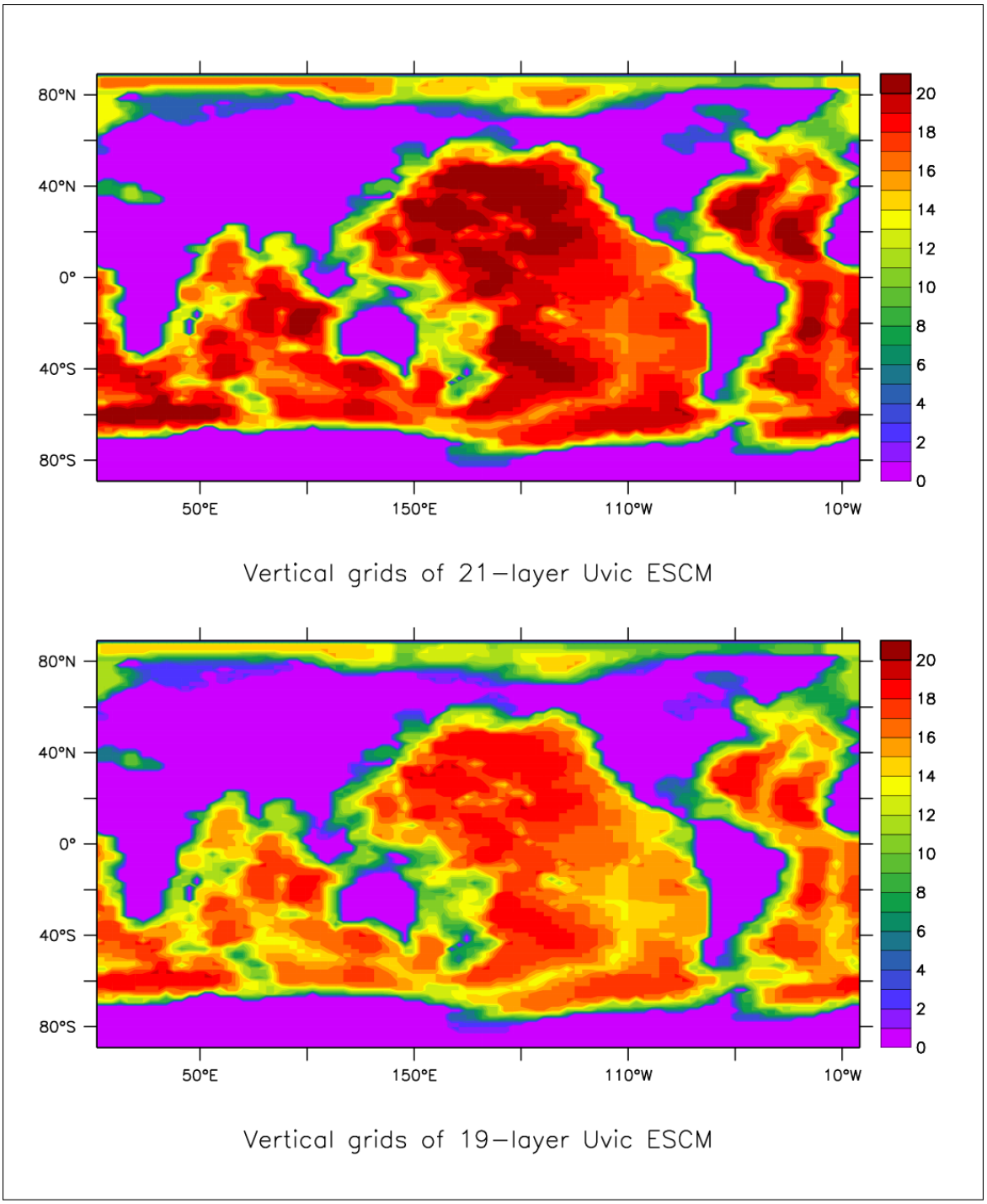


Fig. 2.2 Vertical grid of original (down) and higher vertical resolution (top) Uvic ESCM,

Color bars represent vertical depth levels (different color for each level)

Because of the changes in vertical resolution it was also necessary to modify the initialization data forcing files for data files of salinity, alkalinity, oxygen, and nitrogen, phosphorous, temperature etc. are also modified via MATLAB for higher vertical resolution according to Table 2. Though the first 50 meters are divided into 3 parts, the same values as before are used here to fulfill the new 3 upper layers, in order to keep the new version's initialization forcing as similar as possible to the original one.

# 4 Addition of the ultraviolet radiation (UVB) forcing data

In the older version of Uvic ESCM, UV radiation data is not included. However, this information is required for a photochemistry study. Therefore, UV radiation forcing data was needed for this study. Though solar radiation is already simulated in Uvic ESCM (Weaver, Eby, & Wiebe, 2001), the component is poorly suited for current work , and it is too complicated to separate out the UVB spectrum from the general solar radiation calculations. However, there is good data available to prescribe UVB radiation at the surface of the ocean.

Ultraviolet radiation (UV) is an invisible electromagnetic radiation with a wavelength from 10nm to 400 nm. Among the UV spectrum, UVB (wavelength 280nm-315nm) has the highest energy and is responsible for driving most photochemical reactions (Anderson & Williams, 1999; Sophia C. Johannessen & Miller, 2001; Moran & Zepp, 1997). Thus, UVB radiation can be used to represent the photochemical driver in this study.

The observation dataset of UVB data is originally from gIUV, a global UVB radiation data set for macro ecological studies (Beckmann et al., 2014). The gIUV data set is based on remotely sensed records from NASA's Ozone Monitoring Instrument (Aura-OMI). This dataset is processed from daily UVB measurements, acquired over a period of eight years, into monthly mean UVB data (Fig. 2.3, Beckmann et al., 2014).

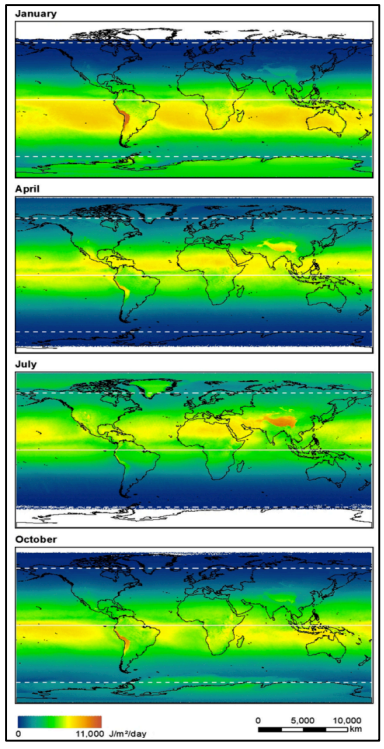


Fig.2.3 Examples of four monthly mean UVB layers: January, April, July and October.

The gIUV datasets are openly available online from the Helmholtz Center for Environmental Research – UFZ (http://www.ufz.de/gluv/index.php?en=32435) in ASCII.

In order to employ gIUV in Uvic ESCM, it is necessary to convert the data from an ASCII to NetCDF format, while re-gridding it to fit the UVic resolution.

Transformation is done in MATLAB to create a global climatology. i.e., 12 separated monthly averaged datasets (from January to December) were combined into a NetCDF file forcing after re-gridding to the Uvic horizontal grid.

# 5 Photochemical degradation model

Diurnal cycles are not simulated here, but are accounted for using a day fraction parameterization,

i.e., a trapezoidal integration function that simulates how much light would reach the ocean during a 24-hour period.

UVB penetration into the water is calculated according to Eq.1, which is modified from the shortwave radiation equation (14) in Keller et al., 2012. Definitions and values of parameters used in the photodegradation model are listed in Table 2.3.

The UVB radiation $\left(\frac{W}{m^2 \cdot s}\right)$ at depth z is:

$$Eq.1 \quad UVB_z = UVB_{z=0} e^{-k_{uw}\tilde{z} - k_{up}\int_0^{\tilde{z}}(P_O + P_D)dz} \times \left(1 + a_i\left(e^{-k_{usi}(h_i + hi_s)} - 1\right)\right)$$

In Eq.1 $UVB_{z=0}$, denoting the downward UVB radiation at the sea surface, is read into the model from the transformed gIUV database. Attenuation of UVB at any depth ($z$) due to seawater, phytoplankton chlorophyll, sea ice, which may be snow covered, is then calculated.

Table 2.3 Parameters used in the RDOM photochemical degradation model

| Parameter | Definition | Value & unit | References |
|---|---|---|---|
| $k_{usi}$ | UVB attenuation factor through ice/snow | 5.0 $m^{-1}$ | Belzile et al., 2000; Govoni et al., 1991 |
| $k_{uw}$ | UVB attenuation factor in water | 0.2 $m^{-1}$ | Smith et al., 1981; Booth et.al, 1997 |
| $k_{up}$ | UVB attenuation factor through phytoplankton | 0.5 $(m*mmol*m^{-3})^{-1}$ | Yentsch, 1982 |
| $h_i$ | Calculated sea ice thickness* | $cm^{-1}$ | Bitz, Holland, Weaver, & Eby, 2001 |
| $a_i$ | Fractional sea ice cover* | $cm^{-1}$ | Bitz, Holland, Weaver, & Eby, 2001 |
| $h_s$ | Calculated snow cover thickness* | $cm^{-1}$ | Bitz, Holland, Weaver, & Eby, 2001 |
| $P_O$ | Amount of phytoplankton* | nmol $m^{-3}$ | Keller, Oschlies, & Eby, 2012 |
| $P_D$ | Amount of diazotroph* | nmol $m^{-3}$ | Keller, Oschlies, & Eby, 2012 |
| $AQY_{RDOM,\ 300nm}$ | Apparent quantum yield of RDOM | $3.8\times10^{-6}$ | Calculate from Stubbins et al., 2012 |
| $a_{RDOM}$ | UVB absorbance coefficient of RDOM | 0.3 $m^{-1}$ | Helms et al., 2013 |

*these parameters are internally calculated by the Uvic ESCM

The basic equation for dissolved matter photochemical degradation is that proposed by Miller et al., 2002. They defined their empirical function based on observations for the photoproduct formation rate and the solar spectral irradiance using the term apparent quantum yield (AQY). AQYs are defined for individual wavelengths and can accommodate differences in light spectra that occur both horizontally and vertically in the ocean. AQY can be defined as:

$$Eq.2 \quad AQY_{\lambda} = \frac{moles\ of\ product}{moles\ of\ photons\ absorbed}$$

In this study, the rate of RDOM photo degradation needs to be determined instead of the production. To do this the spectra representing UVB radiation is determined to be 300nm. Thus, the AQY for RDOM degradation can be modified as followed:

$$Eq.3 \quad AQY_{RDOM,300nm} = \frac{P\ (moles\ of\ reduced)}{N\ (moles\ of\ photons\ absorbed)}$$

As far as I am aware, the AQY for RDOM photo degradation have not been calculated. Thus, a calculation was done based on the experiment result from Stubbins et al., 2012, in which they reported the photo degradation of dissolved black carbon, a fraction of RDOM from deep sea. According to the experiment results, apparently 1000 nmol DBC was degraded during exposure to UVB (with a spectral range from 295 to 365 nm) for 672 hours (28 days).

Since a photon has a distinct energy quanta Ep that is defined by:

$$Eq.4 \quad \mathrm{E_p} = \mathrm{h} \cdot \mathrm{f} = \mathrm{h} \cdot \frac{\mathrm{c}}{\lambda}$$

(with Planck constant h=6.63•10$^{-34}$ [Js]; Speed of light c=2.998•108[m s-1]; Frequency f [s-1]; Wavelength λ [m])

The number of photons Np $(m^{-2} \cdot s^{-1})$ can be calculated by dividing the spectra energy E [W m$^{-2}$] with the distinct photon energy *Ep*:

$$Eq.5 \quad N_p = \frac{E}{E_p} = E \cdot \lambda \cdot 5.03 \cdot 10^{15}$$

The distinct spectral energy value (E) is offered by Dr. A. Stubbins. The photon flux $E_{PF}$ $(\mu mol \cdot m^{-2} \cdot s^{-1})$ can then be determined as:

$$Eq.6 \quad E_{PF} = N_p \,/\, N_A = \frac{E \cdot \lambda \cdot 5.03 \cdot 10^{15}}{6.02 \cdot 10^{17}} = E \cdot \lambda \cdot 0.836 \cdot 10^{-2}$$

(with Avogadro number $N_A$=6.022•10$^{17}$ $\mu mol^{-1}$)

Since the sample was irradiated in 2 L spherical flasks the radiation area (S) is half of the flask's spherical surface area. According to the sphere volume equation, $V = \frac{4\pi r^3}{3}$, and a sphere surface equation $S_{sphere} = 0.4\pi r^2$, it can be calculated that $S = 383[cm^2]$

With the a total irradiation time T=672[h]=2.4192$\times 10^6$ [s], the total photons, P, absorbed by the sample is then:

$$Eq.7 \quad N = E_{PF} \cdot T \cdot S$$

According to Eq.1 and Eq.6, the photon flux $E_{UVB}[nmol \cdot m^{-2} \cdot s^{-1}]$ of $UVB_{300nm}$ radiation at depth z and wavelength $\lambda$=300nm can then be calculated as:

$$Eq.8 \quad E_{UVB}(z) = UVB_z \cdot \lambda \cdot 0.836 \cdot 10^{-2}$$

The absorbance coefficient of RDOM at $UVB_{300nm}$ is from Helms et al., 2013. In that work, water samples from ocean surface to deep ocean (0-3500m) were analyzed for UVB absorbance coefficients, which could represent the RDOM bulk.

The amount of RDOM reduced by photochemical transformation (R) can then be computed as:

$$Eq.9 \quad R = \int E_{UVB}(z) \cdot AQY_{RDOM,300nm} \cdot a_{RDOM} \cdot dz$$

The simulation of refractory DOM circulation and photochemical degradation are carried out based on the 6000-yr spin up model result discussed in Sec.2. The Uvic model starts running with the spin up result by using the data recorded in 'restart.nc' file, which contains the result of 6000-yr steady physical conditions (i.e. salinity, velocity, temperature). Thus, in order to initialize the simulations with the oceanic RDOM/DBC in global uniform concentration (Table 2.1), data of RDOM/DBC was added into 'restart.nc' via Matlab.

Two experimental groups were set up to test the photodegradation of refractory DOM (RDOM) and dissolved black carbon (DBC). Each group has two parallel experiments (RDOM_photo & RDOM_nophoto; DBC_photo & DBC_nophoto) with photodegradation turned on/off. Both simulations are performed for 3500 years.

In this thesis, the parameters of dissolved black carbon (DBC) are set the same as RDOM, as the photochemical properties of DBC (e.g. AQY and absorption efficiency) are not clear yet (Stubbins

et al., 2012). The only difference is the initial uniform concentration (Table. 2.1). The DBC tracer behavior and photodegradation processes are identical to RDOM. The running time of DBC model is 6,000 years. Here only shows the result of simulation and basic analysis.

# Result and Discussion

## 1. UVB penetration and global distribution evaluation

The UVB radiation penetration into the sea is evaluated in the Uvic ESCM. The result is shown in Fig 3.1. From point A to C, the UVB radiation decreases linearly from ~0.05 W/m$^{-2}$ to nearly 0 (2.5e$^{-5}$

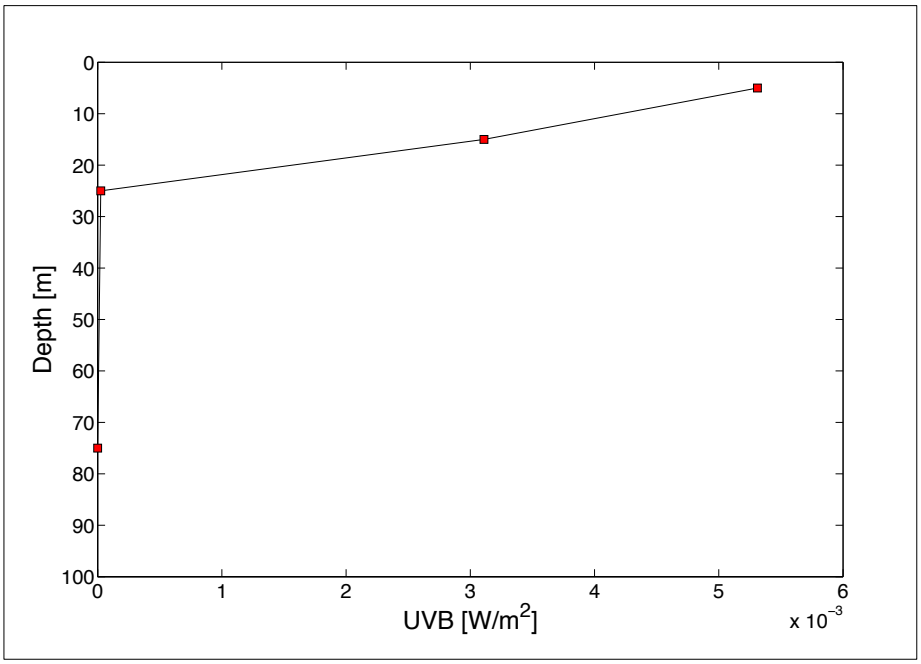


Fig 3.1 Global annual averaged UVB penetration into the ocean

W/m$^{-2}$) while the depth increases from 5m to 25m. The linear decreasing of UVB into water is due to the model resolution. This shows that the UVB radiation and the UVB photochemical reactions can only occur in the upper model layer (~5m to 25m) of the ocean.

The slope of the line is -0.21 [$W \cdot e^{-4}/m^3$]. This rate is the estimated UVB global averaged attenuation rate (0.21 [$W \cdot e^{-4}/m^3$]), which is similar with the UVB attenuation factor through water ($k_{uw}$=0.2 m$^{-1}$, Table 4). The estimated averaged attenuation factor is a little higher than the one in pure water. This is likely due to UVB attenuation through sea ice and phytoplankton.

The global seasonal UVB distribution in the upper ocean layers is shown in Fig 3.2. As UVB radiation amount below 15 meters depth is tiny (Fig 3.1), shown in Fig 3.2 are only 5m (A) and 15m (B) depth levels. Subplot A is the ocean surface UVB distribution which is basically the observations forcing the model, in which the blank space in the top corner and middle bottom are Arctic and Antarctic land

where no satellite data is available due to polar night.

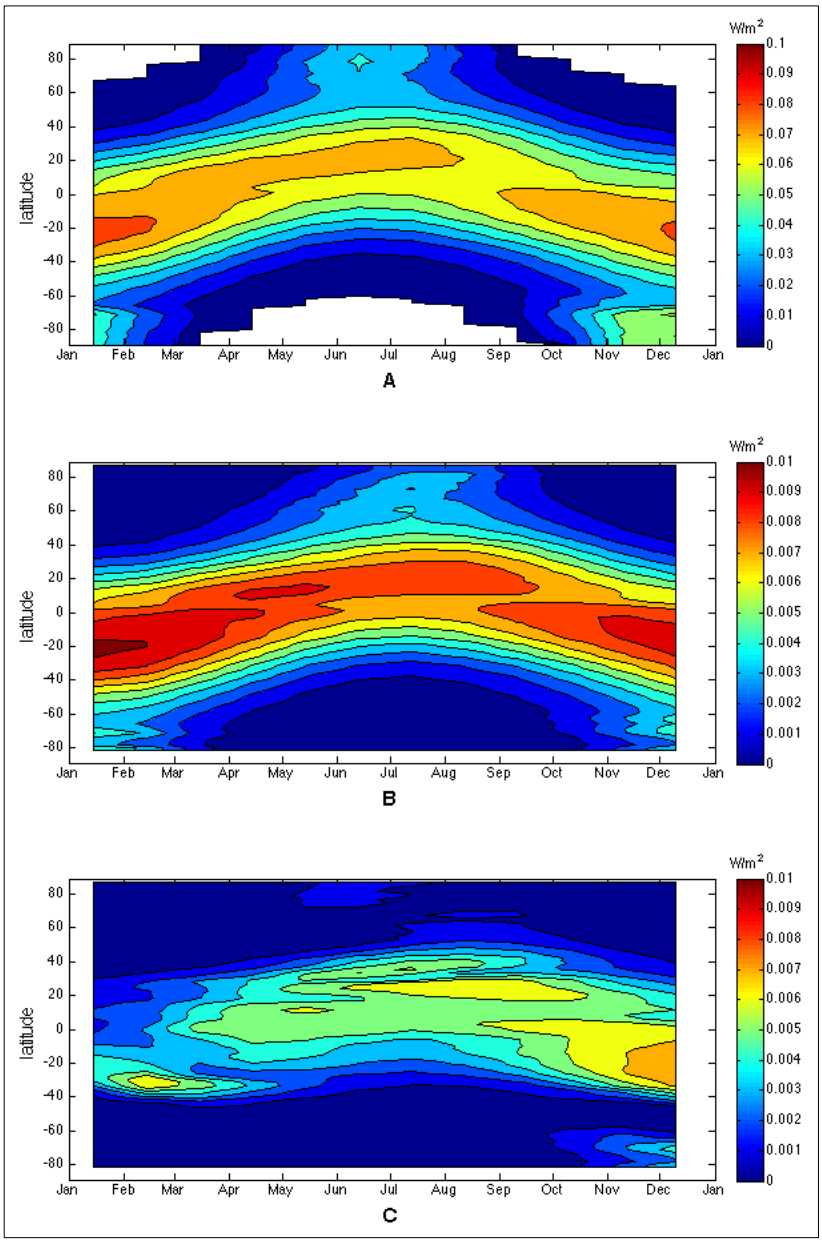


Fig. 3.2. Global annual UVB vertical distribution

A: Ocean surface; B: 5-meters under water; C: 15-meters under water

## 2. Physical evaluation

As mentioned in the Methods section 3, the model's resolution of ocean top layer (~50m) was increased, which also changed the thickness of the other layers. These modifications will affect physical processes, such as ocean circulations. For evaluation, a model spin up of 6000yr was performed, which also is used as a starting point for the UVB research. To assess how the

modifications have changed the model dynamics, comparisons were made between the current 21-layer model (the 'new model') 6000yr spin-up, a 9000yr spin-up from Uvic ESCM 2.9 (19-layer, named the 'old model') and World Ocean Atlas 2009 (WOA09). For the evaluation, the simulated values (both 19-layer version and 21-layer version) were re-gridded onto the observed data (WOA09) grids in Ferret (version 6.82) using the nearest function (@NRST).

Two important physical properties, salinity and temperature, are evaluated here to gain a basic understanding of the differences caused by changing the vertical resolution.

## 2.1 Salinity & Temperature

Globally, the new model does not perform worse when compared to the old model, and it's also reasonable when compared with the WOA09 data (Fig 3.3). From 0 to 500m vertically, the new model salinity result is higher than the other two datasets. Among 800m to 2000m the new model better matches WOA09 than the old model, though it's still far from perfect.

In all the four ocean basins, the new model result among 20m~200m according to the new model results are similar to the observation data/old model profiles. The resolution increasing slightly affects salinity and salinity-related physical properties, such as density and freezing point (UNESCO, 1988).

From 200m~2000m, the new model's performance is acceptable though there are mismatches with the observed values. Overall, the new model generally better simulates global salinity.

However, when come to the bottom layers (3000m to >5000m), both new and old model have deficiencies. Simulated salinity is always lower than observed. It's noteworthy that in the bottom layers, the new model salinity ranges are between the old one and WOA09, suggesting some improvement.

As shown in Fig 3.3, the new model performed superiorly in regards to temperature. Especially at 800m, the new model result better match WOA09. However, in deeper ocean (vertical under 800m), the new model simulates lower temperatures than the observation and the old model simulation.

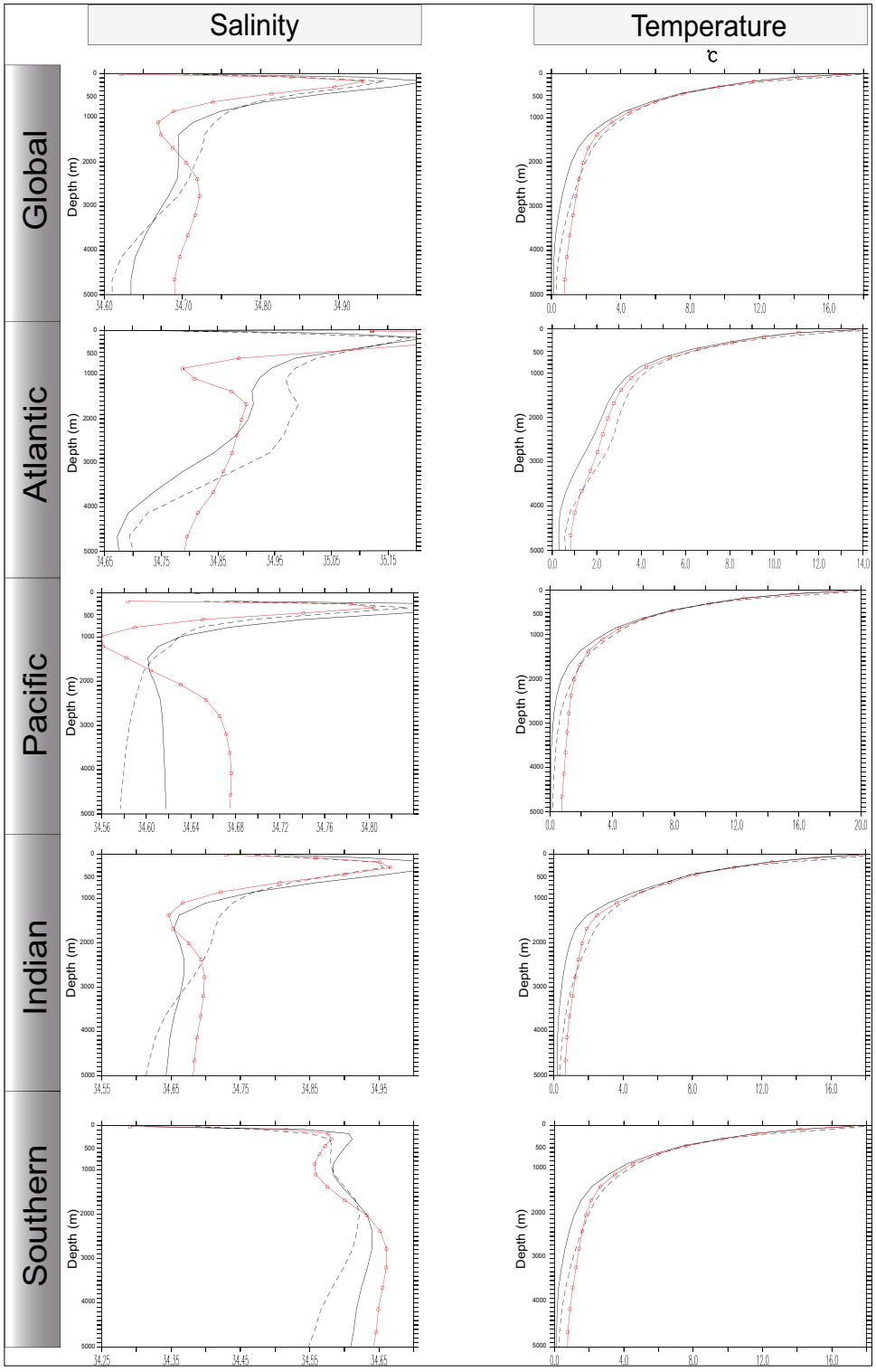


Fig. 3.3 Global and basin-wide averaged vertical profiles of 21-layer model temperature and salinity (solid lines) compared with observations (red line with cubes) and the

## 2.2 Global Currents Evaluation

To further evaluate the basic physical condition in the new model, the currents were compared between the new and old models. The currents were plotted in vector maps in Fig 3.4. As the

current research focuses on the top layers where photochemical reactions happen, 3 layers from the new model and 2 layers from the old one are presented here. As mentioned, the new model has higher resolution in the top 50 meters. Thus, comparisons were performed between layers at similar vertical levels (Fig 3.4).

Additionally, an observational satellite data set of global ocean surface velocity from OSCAR (Ocean Surface Current Analysis Real-time, Bonjean & Lagerloef, 2002) is re-gridded by Ferret and plotted in B3, in order to compare with the 1st layer (5m) velocity from the 21-layer model. OSCAR contains near-surface ocean current estimates, derived using quasi-linear and steady flow momentum equations. The original data are on a 1/3-degree grid with a 5-day resolution. OSCAR is generated by Earth & Space Research Institute(ESR; http://www.esr.org/oscar_index.html).

An overall conclusion can be made that the new model does as well as the old model in simulating global ocean currents. In A1, the new model currents look similar to the old one in B1 both in direction and speed in then Indian Ocean and the Southern Ocean. However, the new model has several mismatches in the Pacific Ocean. Firstly, the North Pacific Drift became weaker. Secondly, around the equator, the direction of North Equatorial Current changed slightly to the east. What these change affects will be discussed in the RDOM degradation section below. Additionally, the eastern part of Equatorial Counter Current was strengthened and shifted northward. The two models performed similarly at about 80 meter (Fig 3.4, A2, B2).

The first layer's velocity (A3) looks compares reasonably well to the OSCAR data (B3). However, differences appear in the Southern Ocean, as the model shows a Southern-Northern direction southern circulation. This could be caused by an insufficiency of good satellite data in the region due to the cloud cover most of the year in the Southern Ocean.

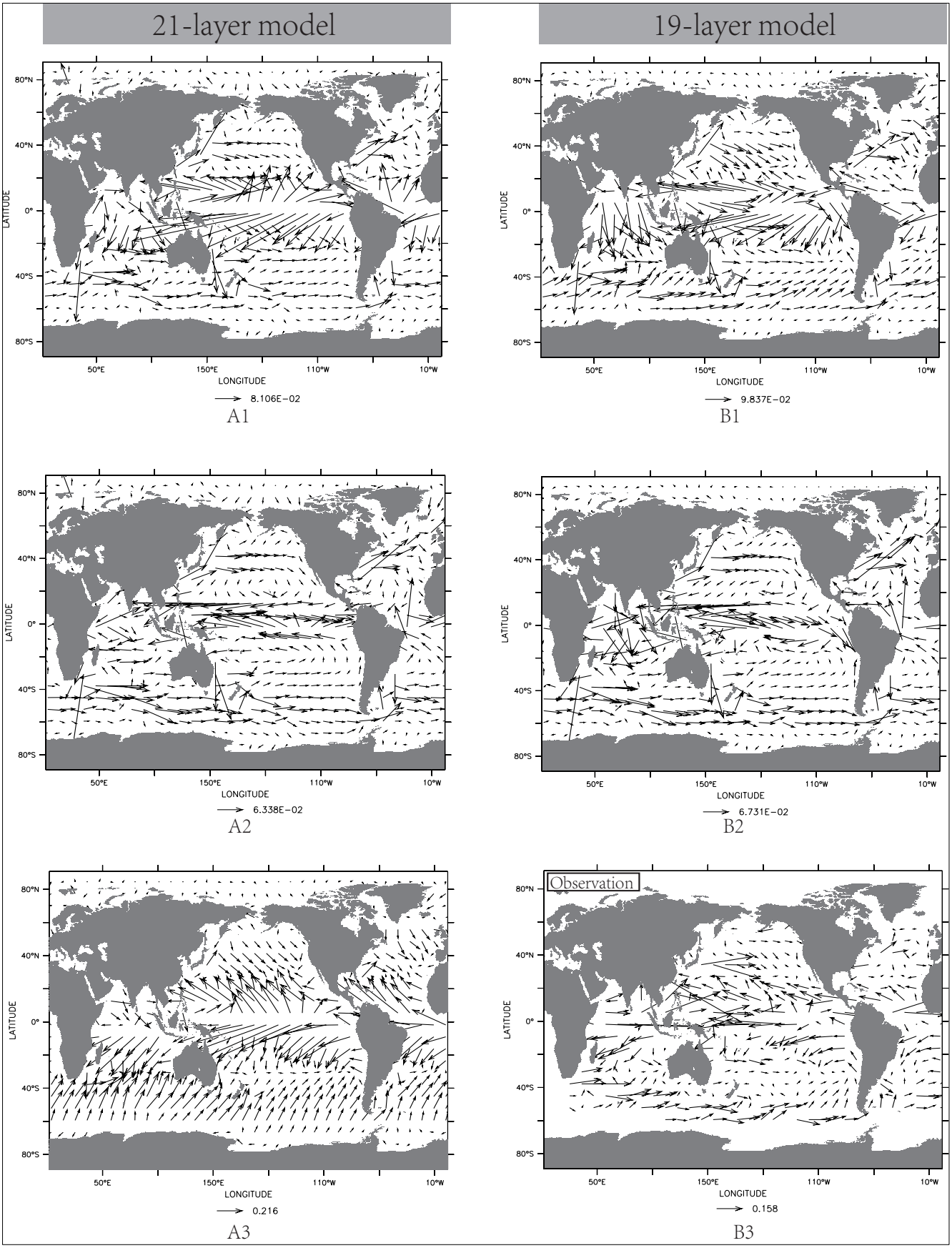


Fig. 3.4 Annual-mean global ocean current vector map at steady state (unit of vector legend: m/s)

A1: 2nd layer (15m); A2: 4th layer (75m); A3: 1st layer (5m)

B1: 1st layer (17.5m); B2: 2nd layer (82.5m); B3: OSCAR surface velocity data

## 2.3 Global Meridional Overturning Circulation (MOC)

The ocean meridional overturning circulation (MOC), which is a system of surface and deep currents encompassing all ocean basins, plays an important role in the global oceanic mass and heat transportation. It transports large amounts of water around the globe, and connects the surface ocean and the deep sea(Schmittner, Chiang, & Hemming, 2013). This system sketched in Fig 3.6 is called “the great conveyor belt”.

At the beginning of the MOC, newly formed deep water in the North Atlantic (North Atlantic Deep Water, NADW) flows southward and crosses the equator (another deep water production region is Antarctic), and eventually enters the Antarctic circumpolar current (ACC) of the Southern Ocean. There, it mixes with other deep water masses like Pacific Deep Water (PDW) to form a new identity, the Circumpolar Deep Water (CDW). Some of this deep water then penetrates northwards, filling the deep waters of the Pacific Ocean and Indian Ocean. Ultimately, these deep waters return to the surface in the upwelling regions (Fig 3.6; Marshall & Speer, 2012). Then the water in the surface Pacific Ocean and Indian Ocean is drifted back to the Atlantic Ocean northerly, during which it mixes with some upwelled water from deep Atlantic Ocean (Fig 3.5).

The stream function of MOC in the higher surface resolution UVic ESCM version is shown in Fig 3.7, where it compares reasonably well with the standard 19-layer Uvic ESCM,.

As the origination of “the great conveyor belt”, the Atlantic MOC (AMOC) consists of four main branches: upwelling processes that transport volume from depth to near the ocean surface, surface currents that transport relatively light water toward high latitudes, deep water formation regions where waters become denser and sink, and deep currents closing the loop(Kuhlbrodt et al., 2007). The AMOC plays an important role due to its role in the large scale re-distribution of heat, $CO_2$ and mass transportation (Lippold et al., 2012). Compared to the normal model, the high resolution model AMOC is acceptable, although the stream function is stronger at equator.

The MOC in higher resolution model is able to meet the basic requirement about tracer transportation and overturning for the current research, and will not be discussed more here. However, analysis and discussion are necessary in further study about the formation and effects of the largely stronger MOC at equator and the MOC in the Pacific in the high resolution model.

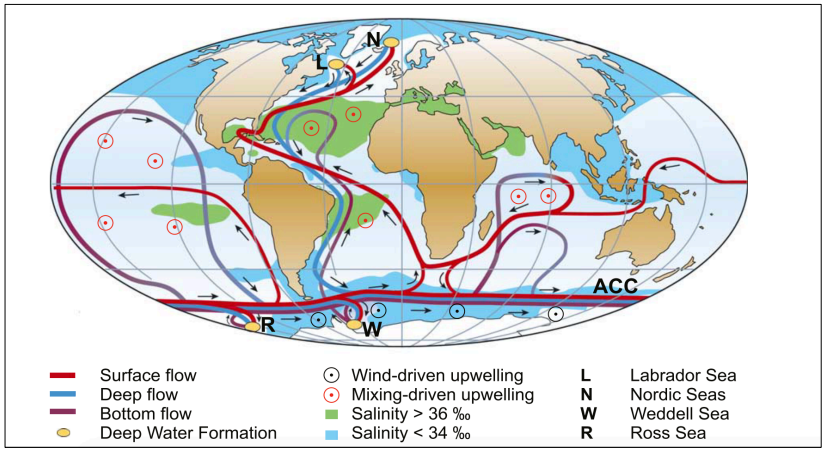


Fig. 3.5 Strongly simplified sketch of the global overturning circulation system (Kuhlbrodt et al., 2007)

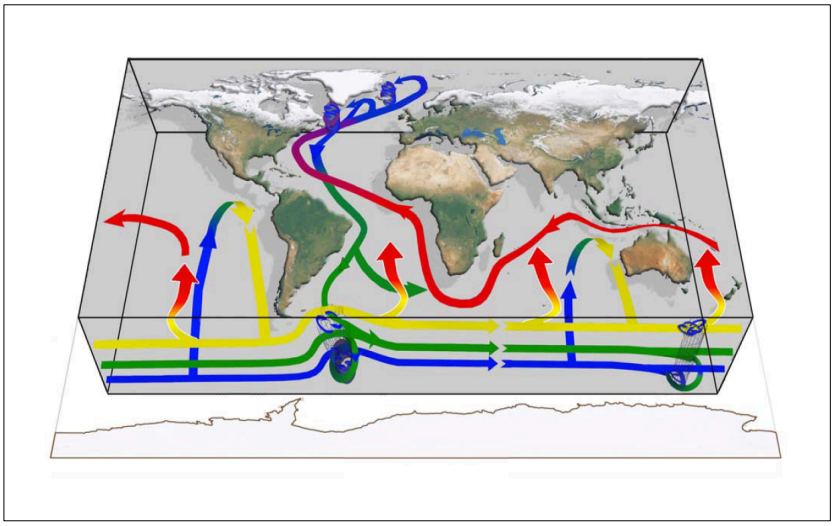

Fig. 3.6 A brief cartoon of oceanic meridional overturning circulation(Marshall & Speer, 2012). Colors schematically indicate the relative density of water masses: warmer mode and thermocline waters (red), upper deep waters (yellow), deep waters including North Atlantic Deep Water (green), and bottom waters (blue).

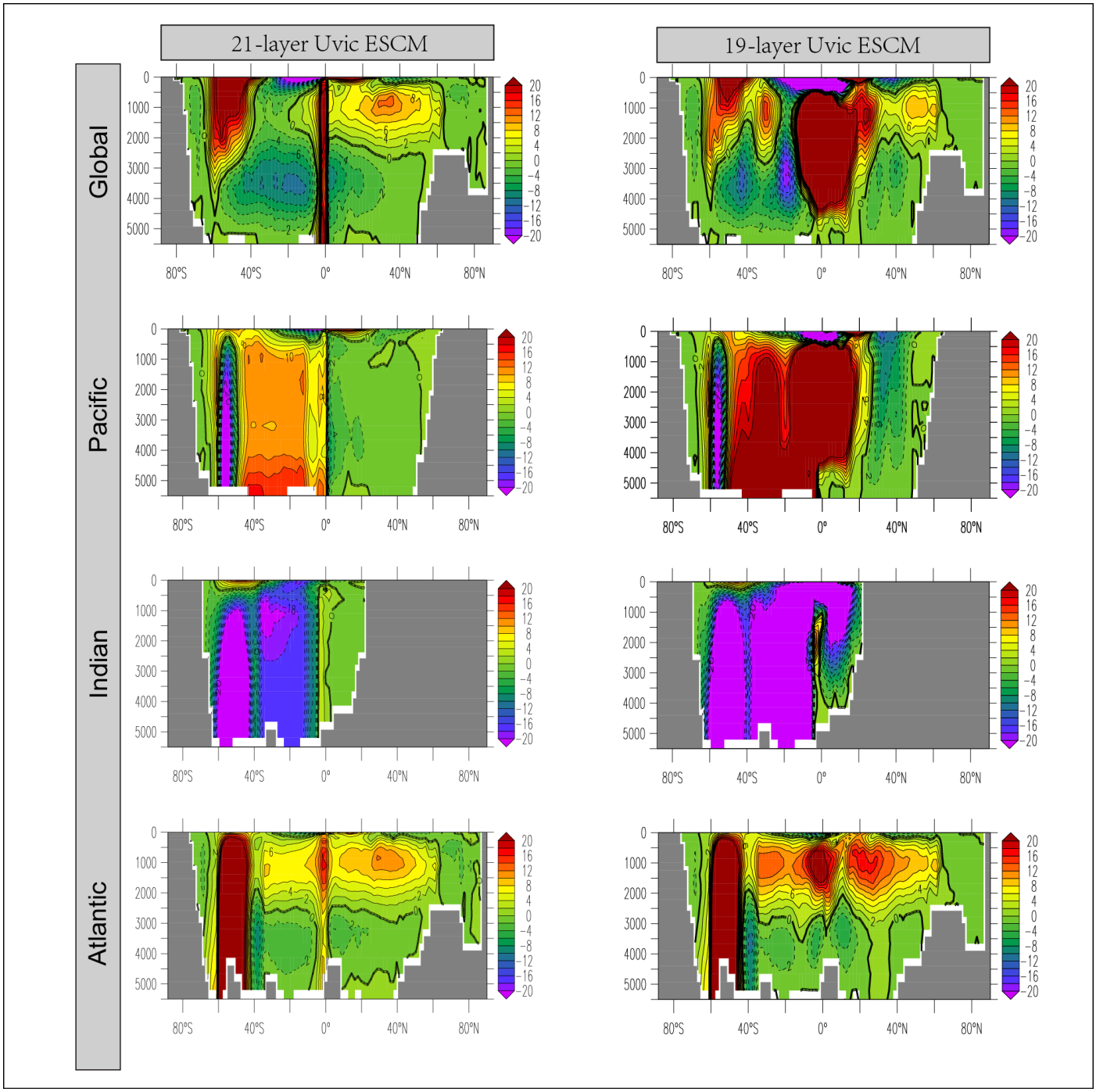


Fig. 3.7 Annual zonal mean values of stream function (Sv) of meridional overturning circulation in global ocean and specified ocean basins

## 3. RDOM photodegradation and global cycling

According to the simulation, it takes 3500 years for 96.3% of the global RDOM pool to be degraded (from $6.736e^{13}$ mol to $2.488e^{12}$ mol, Fig. 3.8).

Stubbins et al. (2012) estimated that the degradation process (without consideration of ocean circulation) may take 30-800 years for the whole DBC pool degradation according to their experiment results. Meanwhile, there are other predictions saying that the lifetime of global RDOM pool is around 15,000 to 16,000 years (Dittmar & Paeng, 2009; Dittmar & Stubbins, 2014; D. Hansell et al., 2009). In the current study, the lifetime of RDOM pool is predicted to be 8,000 to 11,000 years if photo oxidation is the only loss term and an initial uniform distribution is assumed.

Initialized at a uniform concentration ($5e^{-5}$ Molar), the RDOM tracer movement followed global ocean circulation and mixing processes. The RDOM in the upper layers was degraded quickly, meanwhile, the rest in the middle and bottom water mass was only slowly upwelled to the top layer and degraded as it followed the global ocean overturning pathways. This is why the vertical RDOM concentration changed more slowly in the middle-bottom depths than in upper layers (Fig. 3.9).

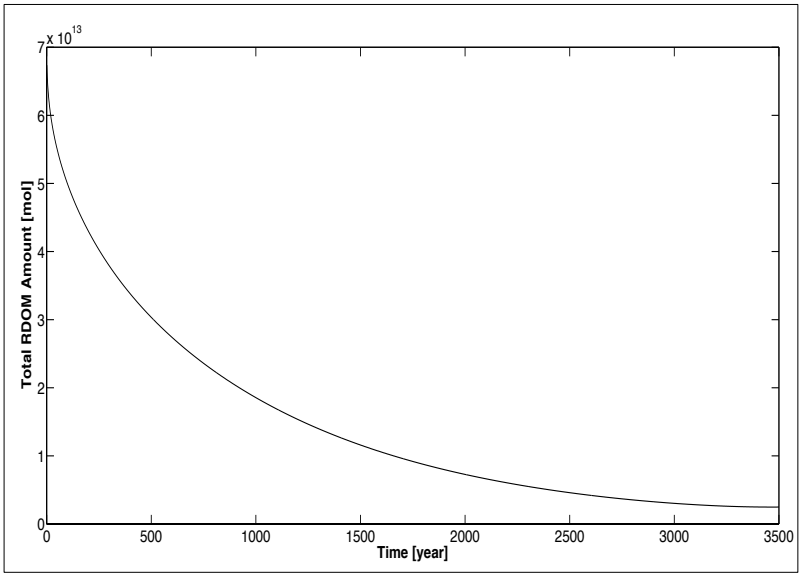


Fig. 3.8 Global RDOM pool change with photochemical degradation

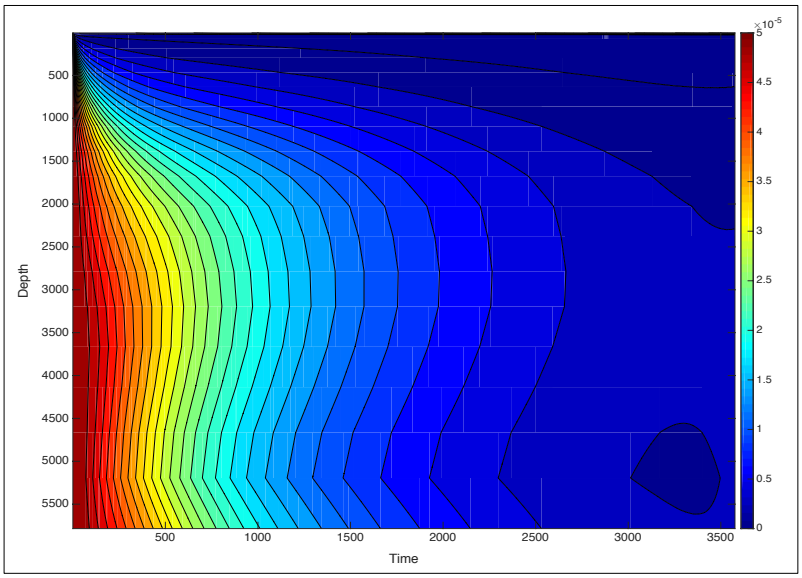


Fig. 3.9 Hovemöller plot of the mean global vertical distribution of RDOM concentration (Molar) during the simulation with degradation.

The final global surface (averaged from 0 to 25m) distribution of RDOM is shown in Fig. 3.10 (RDOM_nophoto). After 3500-yr mixing and overturning, the tracer gathers at tropical and subtropical zones. Meanwhile, the RDOM gethered at the upwelling zones (Fig. 3.10, Kuhlbrodt et al., 2007). It can also been seen that the Atlantic Ocean surface has a high concentration of RDOM. Some of the RDOM was finally transported to the surface of the Atlantic Ocean by the MOC surface flow (Fig 3.5), or other physical processes, e.g., diffusion.

Fig 3.11 shows the *in situ* monthly photodegradation reaction rate during the first model year (when RDOM was evenly distributed throught the ocean) at the ocean surface (5m). According to the UVB distribution (Fig 3.2), the RDOM degradation happened mainly in the tropics and subtropics. In the polar zones, photodegradation occurred only during the polar day period and disappeared during the polar night period.

The global distribution of RDOM_photo and RDOM_nophoto after 3500-yr is shown in Fig 3.12. In Fig 3.12 series B, it can be seen that after 3500-yr simulation, the RDOM tracer is concentrated between 40°N and 40°S and depths of 0m to 1,000m.

In Fig 3.12 series A, it can be seen that with photodegradation, the Pacific deep water contains relatively more RDOM than the other basins whose concentrations are nearly zero. This is because the Pacific Ocean deep water is the oldest water mass (Koeve, Wagner, Kähler, & Oschlies, 2015), i.e., it takes a long time before this RDOM is upwelled into the surface and can be photodegradated.

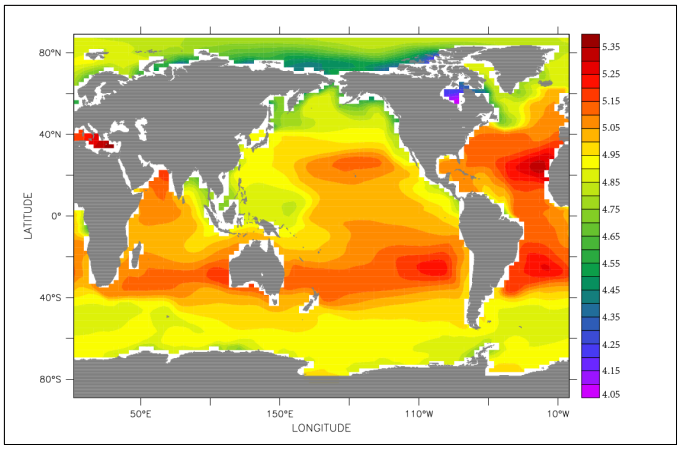


Fig. 3.10 Estimated Global Ocean Surface Distribution of RDOM after 3500-yr Running (RDOM_nophoto, $10^{-5}$ Molar)

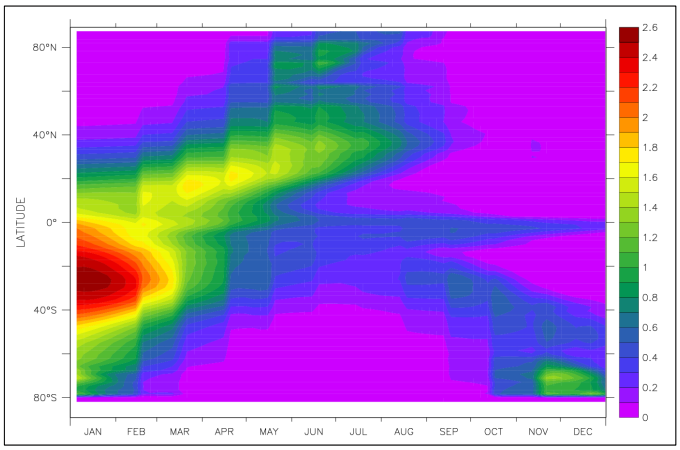


Fig. 3.11 Global *in situ* surface RDOM photodegradation rate (RDOM_photo, $10^{-15}$ Molar/s)

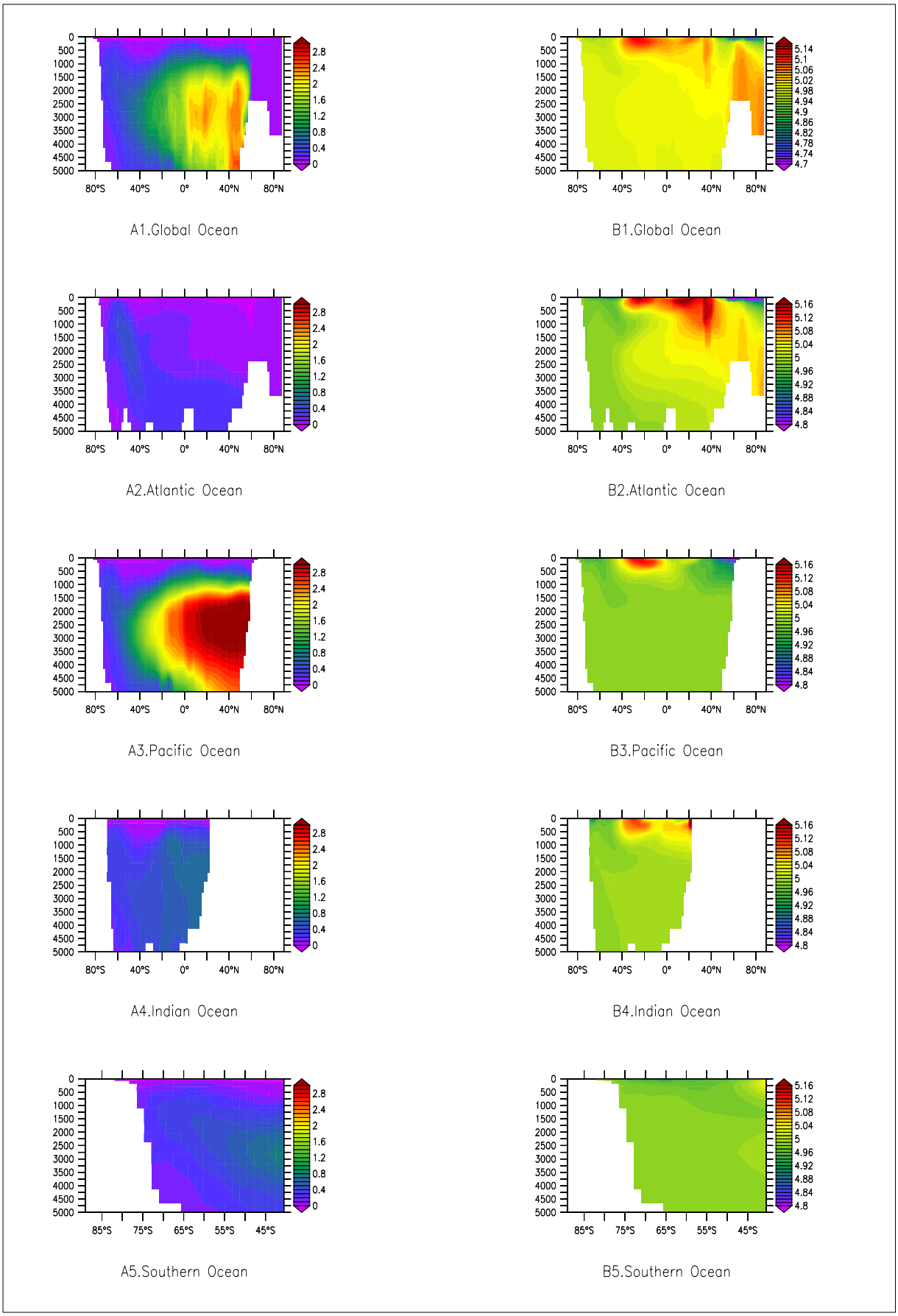


Fig. 3.12 Simulated RDOM annual zonal averaged vertical distribution (Molar) along latitude with (series A) & without (series B) photodegradation at 6500-yr

Based on the simulation in current research, the global RDOM pool will be entirely photodegradated in 8,000 to 11,000 years because of global ocean circulation. This result is similar to the reported average apparent radio carbon age of RDOM, 4,000–6,000 years (Bauer, Williams, & Druffel, 1992). Meanwhile, the current simulated life time of RDOM pool is 5 to 10 times that of thermohaline circulation, which has been estimated to be 550–2,000yr (Chapman, Shackleton, & Chapman, 2000; Primeau, 2005). This means that RDOM may travel throughout the global ocean 5 to 10 times before being photoxidized.

However, it has been reported that the RDOM pool is stable with a uniform concentration (=~40μM; C. A. Carlson & Ducklow, 1995; Dittmar & Stubbins, 2014; D. Hansell et al., 2009; Ogawa & Tanoue, 2003). An incubation experiment suggets that the rate of labile DOM transformation into RDOM is 0.5 to 0.6 Gt C per year (Fabry et al., 2005), however the current simulated average photodegradation is about $2.25\times10^5$t C, which is much less than the production rate. Thus, if RDOM concentrations are unchanging then the sources and sinks must equal each other.

A potentially crucial RDOM generation method is sedimentation of POM ($0.1\times10^9$t C per year) via the biological pump and the transformation from LDOM to RDOM by microbial carbon pump (MCP), meanwhile these two processes are connected by microbial loop, whereby DOM is taken up by hetero- trophic microorganisms and transported to the grazing food web (Jiao et al., 2010). Three major pathways have been identified in the microbial carbon pump: direct exudation of microbial cells during production and proliferation; viral lysis of microbial cells to release microbial cell wall and cell surface macromolecules; and POM degradation. The microbial loop is a general interaction in which DOM is utilized as an energy source, starting with DOM consumed by bacteria via respiration, which makes its way through various trophic levels ultimately to the highest trophic levels.

Besides, approximately 0.5% of the net primary production on the continents ($2.4\times10^8$t C per year) is transported toward the ocean in the form of organic matter via rivers (Hedges, Keil, & Benner, 1997), tidal pumping (Dittmar & Koch, 2006) or as aerosols (Hernes & Benner, 2006). This flux could also play a significant role in balancing the turnover of refractory (Dittmar & Stubbins, 2014).

## 4. Dissolved Black Carbon

The global DBC pool was nearly entirely degradated after 6000yr. This simulated result is much longer than the estimated life duration of 1600 years based on photochemical experiment results

in the surface ocean without ocean circulation being considered (Stubbins et al., 2012).

As metioned in the Method section, some of the photochemical properties of RDOM and DBC are extracted from the laboratory result of Stubbins et al. (2012). The large variation between lab work estimation and ESCM result suggests that the photochemical degradation of DBC in global ocean is determined by multiple ocean situations, such as physical processes and biological processes, but not only by UV radiation and molecular photochemical properties.

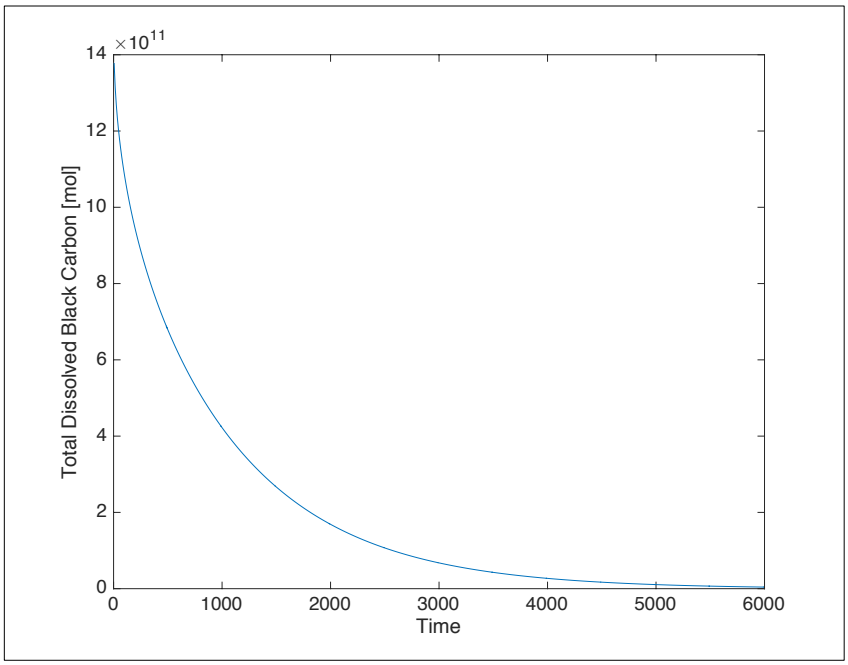


Fig. 3.13 Global DBC pool change with photochemical degradation

# Conclusions and future research directions

In this thesis, the photochemical degradation of RDOM and DBC are investigated. The work was performed on Uvic ESCM, a numerical Earth system model of intermediate complexity.

The model's vertical resolution in the top 50m ocean surface was increased (Table. 2.2), and the physical evaluation of the higher resolution model was determined to be reasonable. A new tracer for RDOM/DBC and related functions of photochemistry were added into the modified model. Meanwhile, UV radiation database and related numerical functions were added into the Uvic ESCM as the forcing data for the photochemistry processes. Afterwards, the simulated photochemical degradation and global circulation of RDOM was successfully performed with the modified Uvic ESCM.

This study shows that photodegradation is influenced by oceanic physical transportation (which controls the distribution of the tracer and its exposure to UVB at the surface) and UVB radiation (which is affected by depth and season depending on the latitude). According to the result, it is concluded that the photochemical degradation mainly happened around 40°N to 40°S at 0 to 30m underwater. The RDOM tracer gathered (with degradation off) at the upwelling surface regions, especially near the equator. The highest degradation rate (with degradation on) also occurred at these regions. Meanwhile, the lowest UVB radiation regions are the polar areas.

After a 3,500-yr simulation, more than 90% of RDOM was degraded, which suggested the life time of global RDOM could be 8,000 to 11,000 years. Meanwhile, the DBC life time was 6,000 years in the simulations. Both results were different from the estimations based on lab experiments.

There are also some hypotheses to be studied and tested in the future:

1) More analysis is needed about the quantities and qualities of RDOM sources and consumption pathways. As discussed above, there should exist input sources of RDOM into the ocean, which keeps the RDOM pool from changing in the global ocean. These sources could be terrestrial fresh water injections, bacterial production, etc. Meanwhile, consumption, such as heat induction near hydrothermal vent regions (Dittmar & Koch, 2006) and sedimentation, should also be investigated in details.

2) The ozone holes will enhance the UV light entrance to the earth surface (Whitehead, De Mora, & Demers, 2000). Will that influence the photodegradation of RDOM and it's role in global

carbon storage and climate change?

3) Data should be collected to better understand the photochemical properties of DBC and RDOM. The absence of these parameters makes it difficult to simulate DBC and RDOM photochemical behavior.

# Acknowledgment

This thesis was supported and founded by the group Marine Biogeochemical Modeling of GEOMAR Helmholtz Centre for Ocean Research Kiel. I would like to thank my supervisors, Dr. David Keller and Pr. Andreas Oschlies for the thesis opportunity and all the advices you gave me. A special and heartful gratitude to David, not only for going above and beyond being my supervisor and giving me advices and support with so much patience, but also for helping me growing up from a zero beginner to a junior modeler. Thank you to everyone else that helped me with this thesis which would not have finished without these people: Dr. Markus Pahlow, Dr. Christopher Somes, Dr. Bei Su and Mr. Yuming Feng. I really felt myself being at home in the BM group, and people in this group made me feel warm. Besides, I would like to give my sincere gratitude to Dr. Aron Stubbins for offering the distinct spectral energy value, which is crucial for the key function calculating AQY.

Sincere thanks should go to my friends who have supported me all the way during my Master studying: Mr. Chi Guan, Mr. Ruiyan Zhang, Mr. Wenbin Cui, Mr. Ding Jin, Ms. Yimei Zhang, Mr. Kang Ding, Mr. Runsheng Chen and Mr. Yujia Jin. Meanwhile, I would like to give my heartfelt thanks to Mr. Jiannan Ma, Ms. Bingqing Yan, Mr. Ou Lu and Dr. Min Luo. I'm so powerful and enthusiastic with you guys standing by me. I'm also deeply indebt to my girlfriend, Ms. Peixuan Bao, for her encouragement and accompanying. Thank you to all my classmates in Master of Biological Oceanography 2013.

Last but not least, thank you my parents and my family, who raise me up and always support me heart and soul.

# References


Anderson, T. R., & Williams, P. J. L. B. (1999). A one-dimensional model of dissolved organic carbon cycling in the water column incorporating combined biological-photochemical decomposition. *Global Biogeochemical Cycles*, *13*(2), 337. http://doi.org/10.1029/1999GB900013

Bauer, J. E., Williams, P. M., & Druffel, E. R. M. (1992). C-14 Activity of Dissolved Organic Carbon Fractions in the North-Central Pacific and Sargasso Sea. *Nature*, *357*(6380), 667–670.

Beckmann, M., Václavík, T., Manceur, A. M., Šprtová, L., von Wehrden, H., Welk, E., & Cord, A. F. (2014). glUV: a global UV-B radiation data set for macroecological studies. *Methods in Ecology and Evolution*, *5*(4), 372–383. http://doi.org/10.1111/2041-210X.12168

Belzile, C., Johannessen, S. C., Gosselin, M., Demers, S., & Miller, W. L. (2000). Ultraviolet attenuation by dissolved and particulate constituents of first-year ice during late spring in an Arctic polynya. *Limnology and Oceanography*, *45*(6), 1265–1273. http://doi.org/10.4319/lo.2000.45.6.1265

Benner, R., & Biddanda, B. (1998). Photochemical transformations of surface and deep marine dissolved organic matter: Effects on bacterial growth. *Limnology and Oceanography*, *43*(6), 1373–1378. http://doi.org/10.4319/lo.1998.43.6.1373

Benner, R., & Kaiser, K. (2011). Biological and photochemical transformations of amino acids and lignin phenols in riverine dissolved organic matter. *Biogeochemistry*, *102*(1), 209–222. http://doi.org/10.1007/s10533-010-9435-4

Bitz, C. M., Holland, M. M., Weaver, A. J., & Eby, M. (2001). Simulating the ice-thickness distribution in a coupled climate model. *Journal of Geophysical Research*, *106*(C2), 2441. http://doi.org/10.1029/1999JC000113

Bonjean, F., & Lagerloef, G. S. E. (2002). Diagnostic model and analysis of the surface currents in the tropical Pacific Ocean. *Journal of Physical Oceanography*, *32*(10), 2938–2954. http://doi.org/10.1175/1520-0485(2002)032<2938:DMAAOT>2.0.CO;2

Booth, C., & Morrow, J. (1997). The penetration of UV into natural waters. *Photochemistry and Photobiology*, *65*(2), 254–257. http://doi.org/10.1111/j.1751-1097.1997.tb08552.x

Carlson, C. a. (2002). Production and Removal Processes. *Biogeochemistry of Marine Dissolved Organic Matter*, (805), 139–151. http://doi.org/10.1016/B978-012323841-2/50006-3

Carlson, C. A., & Ducklow, H. W. (1995). Dissolved organic carbon in the upper ocean of the central equatorial Pacific Ocean, 1992: Daily and finescale vertical variations. *Deep-Sea Research Part II*, *42*(2-3), 639–656. http://doi.org/10.1016/0967-0645(95)00023-J

Carlson, C. A., Ducklow, H. W., & Michaels, A. F. (1994). Annual flux of dissolved organic carbon from the euphotic zone in the northwestern Sargasso Sea. *Nature*, *371*(6496), 405–408. http://doi.org/10.1038/371405a0

Chapman, M. R., Shackleton, N. J., & Chapman, M. R. (2000). Evidence of 550-year and 1000-year cyclicities in North Atlantic circulation patterns during the Holocene. *The Holocene*, *10*(3), 287–291. http://doi.org/10.1191/095968300671253196

Christian, J. R., & Anderson, T. R. (2002). Chapter 16 - Modeling {DOM} Biogeochemistry. In *Biogeochemistry of Marine Dissolved Organic Matter* (pp. 717–755). http://doi.org/http://dx.doi.org/10.1016/B978-012323841-2/50018-X

Del Giorgio, P., & Williams, P. (2005). *Respiration in Aquatic Ecosystems*. (P. del Giorgio & P. Williams, Eds.), *Respiration in Aquatic Ecosystems*. Oxford University Press. http://doi.org/10.1093/acprof:oso/9780198527084.001.0001

Dittmar, T., & Kattner, G. (2003). The biogeochemistry of the river and shelf ecosystem of the Arctic Ocean: a review. *Marine Chemistry*, *83*(3-4), 103–120. http://doi.org/10.1016/S0304-4203(03)00105-1

Dittmar, T., & Koch, B. P. (2006). Thermogenic organic matter dissolved in the abyssal ocean. *Marine Chemistry*, *102*(3-4), 208–217. http://doi.org/10.1016/j.marchem.2006.04.003

Dittmar, T., & Paeng, J. (2009). A heat-induced molecular signature in marine dissolved organic matter. *Nature Geoscience*, *2*(3), 175–179. http://doi.org/10.1038/ngeo440

Dittmar, T., & Stubbins, A. (2014). *Dissolved Organic Matter In Aquatic Systems*. *Treatise on Geochemistry* (2nd ed., Vol. 12). Elsevier Ltd. http://doi.org/10.1016/B978-0-08-095975-7.01010-X

Druffel, E. R. M., Williams, P. M., Bauer, E., & Ertel, J. R. (1992). Cycling of Dissolved and Particulate Organic Matter in the Open Ocean. *Journal of Geophysical Researh*, *97*, 15,639 – 15,659. http://doi.org/10.1029/92JC01511

Fabry, V. J., Orr, J. C., Aumont, O., Bopp, L., Doney, S. C., Feely, R. A., … Yool, A. (2005). Anthropogenic ocean acidification over the twenty-first century and its impact on calcifying organisms. *Nature*, *437*(7059), 681–6. http://doi.org/10.1038/nature04095

Fichot, C. G., & Miller, W. L. (2010). An approach to quantify depth-resolved marine photochemical fluxes using remote sensing: Application to carbon monoxide (CO) photoproduction. *Remote Sensing of Environment*, *114*(7), 1363–1377. http://doi.org/10.1016/j.rse.2010.01.019

Field, C. B., Behrenfeld, M. J., & Randerson, J. T. (1998). Primary Production of the Biosphere : Integrating Terrestrial and Oceanic Components, *281*(July), 237–240.

Gogou, A., & Repeta, D. J. (2010). Particulate-dissolved transformations as a sink for semi-labile

dissolved organic matter: Chemical characterization of high molecular weight dissolved and surface-active organic matter in seawater and in diatom cultures. *Marine Chemistry*, *121*(1-4), 215–223. http://doi.org/10.1016/j.marchem.2010.05.001

Govoni, J. W., & Perovich, D. K. (1991). Absorption coefficients of ice from 250 to 400nm. Retrieved from http://www.sengpielaudio.com/Calculations03.htm

Guan, L. L., & Kamino, K. (2001). Bacterial response to siderophore and quorum-sensing chemical signals in the seawater microbial community. *BMC Microbiology*, *1*, 27. http://doi.org/http://www.biomedcentral.com/1471-2180/1/27

Häder, D. P., Kumar, H. D., Smith, R. C., & Worrest, R. C. (1998). Effects on aquatic ecosystems. *Journal of Photochemistry and Photobiology B: Biology*, *46*(1-3), 53–68. http://doi.org/10.1016/S1011-1344(98)00185-7

Hansell, D. A., & Carlson, C. A. (1998). Net community production of dissolved organic carbon. *Global Biogeochemical Cycles*, *12*(3), 443–453. http://doi.org/10.1029/98GB01928

Hansell, D. A., Carlson, C. A., Repeta, D. J., & Schlitzer, R. (2009). Dissolved Organic Matter in the Ocean A Controversy Stimulates New Insights. *Oceanography*, *22*(4), 202–211. http://doi.org/10.5670/oceanog.2009.109

Hansell, D. A., Carlson, C. A., & Schlitzer, R. (2012). Net removal of major marine dissolved organic carbon fractions in the subsurface ocean, *26*(November 2011), 1–9. http://doi.org/10.1029/2011GB004069

Hansell, D., Carlson, C. A., Repeta, D. J., & Schlitzer, R. (2009). Dissolved Organic Matter in the Ocean. *Oceanography*, *22*(4), 202–11. http://doi.org/10.5670/oceanog.2009.109

Hedges, J. I., Keil, R. G., & Benner, R. (1997). What happens to terrestrial organic matter in the ocean? *Organic Geochemistry*, *27*(5-6), 195–212. http://doi.org/10.1016/S0146-6380(97)00066-1

Helms, J. R., Stubbins, A., Perdue, E. M., Green, N. W., Chen, H., & Mopper, K. (2013). Photochemical bleaching of oceanic dissolved organic matter and its effect on absorption spectral slope and fluorescence. *Marine Chemistry*, *155*, 81–91. http://doi.org/10.1016/j.marchem.2013.05.015

Hernes, P. J., & Benner, R. (2006). Terrigenous organic matter sources and reactivity in the North Atlantic Ocean and a comparison to the Arctic and Pacific oceans. *Marine Chemistry*, *100*(1-2), 66–79. http://doi.org/10.1016/j.marchem.2005.11.003

Hopkinson, C. S., & Vallino, J. J. (2005). Efficient export of carbon to the deep ocean through dissolved organic matter. *Nature*, *433*(7022), 142–145. http://doi.org/10.1038/nature03191

Jiao, N., Herndl, G. J., Hansell, D. A., Benner, R., Kattner, G., Wilhelm, S. W., … Azam, F. (2010). Microbial production of recalcitrant dissolved organic matter: long-term carbon storage in the global ocean. *Nature Reviews Microbiology*, *8*(8), 593–599. http://doi.org/10.1038/nrmicro2386

Johannessen, S. C. (2003). Calculation of UV attenuation and colored dissolved organic matter absorption spectra from measurements of ocean color. *Journal of Geophysical Research*, *108*(C9). http://doi.org/10.1029/2000JC000514

Johannessen, S. C., & Miller, W. L. (2001). Quantum yield for the photochemical production of dissolved inorganic carbon in seawater. *Marine Chemistry*, *76*(4), 271–283. http://doi.org/10.1016/S0304-4203(01)00067-6

Keller, D. P., & Hood, R. R. (2011). Modeling the seasonal autochthonous sources of dissolved organic carbon and nitrogen in the upper Chesapeake Bay. *Ecological Modelling*, *222*(5), 1139–1162. http://doi.org/10.1016/j.ecolmodel.2010.12.014

Keller, D. P., & Hood, R. R. (2013). Comparative simulations of dissolved organic matter cycling in idealized oceanic, coastal, and estuarine surface waters. *Journal of Marine Systems*, *109-110*, 109–128. http://doi.org/10.1016/j.jmarsys.2012.01.002

Keller, D. P., Oschlies, a., & Eby, M. (2012). A new marine ecosystem model for the University of Victoria earth system climate model. *Geoscientific Model Development*, *5*(5), 1195–1220. http://doi.org/10.5194/gmd-5-1195-2012

Koehler, B., Landelius, T., Weyhenmeyer, G. a, Machida, N., & Tranvik, L. J. (2014). Sunlight-induced carbon dioxide emissions from inland waters. *Global Biogeochemical Cycles*, *28*, 696–711. http://doi.org/10.1002/2014GB004850.Received

Koeve, W., Wagner, H., Kähler, P., & Oschlies, a. (2015). <sup>14</sup>C-age tracers in global ocean circulation models. *Geoscientific Model Development*, *8*(7), 2079–2094. http://doi.org/10.5194/gmd-8-2079-2015

Krogh, A., & Keys, A. (1934). METHODS FOR THE DETERMINATION OF ORGANIC CARBON AND NITROGEN DISSOLVED I NTRODUCTION Certain problems in the nutrition of marine animals and in the gen . eral economy of organic life in the sea involve the determination of or material determined by combus. *The Biological Bulletin*, *67*, 132–144.

Kuhlbrodt, T., Griesel, a, Montoya, M., Levermann, a, Hofmann, M., & Rahmstorf, S. (2007). On the driving processes of the Atlantic meridional overturning circulation. *Atlantic*, *45*(2004), RG2001. http://doi.org/10.1029/2004RG000166.1.INTRODUCTION

Lee, Z., Hu, C., Shang, S., Du, K., Lewis, M., Arnone, R., & Brewin, R. (2013). Penetration of UV-visible solar radiation in the global oceans: Insights from ocean color remote sensing. *Journal of Geophysical Research: Oceans*, *118*, 4241–4255. http://doi.org/10.1002/jgrc.20308

Lippold, J., Luo, Y., Francois, R., Allen, S. E., Gherardi, J., Pichat, S., … Schulz, H. (2012). Strength and geometry of the glacial Atlantic Meridional Overturning Circulation. *Nature Geoscience*, *5*(11), 813–816. http://doi.org/10.1038/ngeo1608

Marshall, J., & Speer, K. (2012). Closure of the meridional overturning circulation through Southern Ocean upwelling. *Nature Geoscience*, *5*(3), 171–180. http://doi.org/10.1038/ngeo1391

Miller, W. L., Moran, M. A., Sheldon, W. M., Zepp, R. G., & Opsahl, S. (2002). Determination of apparent quantum yield spectra for the formation of biologically labile photoproducts. *Limnology and Oceanography*, *47*(2), 343–352. http://doi.org/10.4319/lo.2002.47.2.0343

Mopper, K., & Kieber, D. J. (2002). Photochemistry and the Cycling of Carbon, Sulfur, Nitrogen and Phosphorus. *Biogeochemistry of Marine Dissolved Organic Matter*, 455–489. http://doi.org/10.1016/B978-012323841-2/50011-7

Mopper, K., Zhou, X., Kieber, R. J., Kieber, D. J., Sikorski, R. J., & Jones, R. D. (1991). Photochemical degradation of dissolved organic carbon and its impact on the oceanic carbon cycle. *Nature*, *353*(6339), 60–62. http://doi.org/10.1038/353060a0

Moran, M. A., & Zepp, R. G. (1997). Role of photoreactions in the formation of biologically labile compounds from dissolved organic matter. *Limnology and Oceanography*, *42*(6), 1307–1316. http://doi.org/10.4319/lo.1997.42.6.1307

Nealson, K. H., & Hastings, J. W. (2006). Quorum Sensing on a Global Scale: Massive Numbers of Bioluminescent Bacteria Make Milky Seas. *Applied and Environmental Microbiology*, *72*(4), 2295–2297. http://doi.org/10.1128/AEM.72.4.2295-2297.2006

Nebbioso, A., & Piccolo, A. (2013). Molecular characterization of dissolved organic matter (DOM): A critical review. *Analytical and Bioanalytical Chemistry*, *405*(1), 109–124. http://doi.org/10.1007/s00216-012-6363-2

Ogawa, H., & Tanoue, E. (2003). Dissolved Organic Matter in Oceanic Waters. *Journal of Oceanography*, *59*(2), 129–147. http://doi.org/10.1023/A:1025528919771

Passow, U., Alldredge, A. L., & Logan, B. E. (1994). The role of particulate carbohydrate exudates in the flocculation of diatom blooms. *Deep Sea Research Part I: Oceanographic Research Papers*, *41*(2), 335–357. http://doi.org/10.1016/0967-0637(94)90007-8

Primeau, F. (2005). Characterizing Transport between the Surface Mixed Layer and the Ocean Interior with a Forward and Adjoint Global Ocean Transport Model. *Journal of Physical Oceanography*, *35*(4), 545–564. http://doi.org/10.1175/JPO2699.1

Schmittner, A., Chiang, J. C. H., & Hemming, S. R. (2013). Introduction: The Ocean's Meridional Overturning Circulation. *Ocean Circulation: Mechanisms and Impacts - Past and Future Changes of Meridional Overturning*, 1–4. http://doi.org/10.1029/173GM02

Sharp, J. H. (2002). Chapter 2\; Analytical Methods for Total DOM Pools.pdf. In *Biogeochemistry of Marine Dissolved Organic Matter* (p. 774). Retrieved from https://books.google.co.il/books?hl=iw&lr=&id=D6TMKZOgldAC&oi=fnd&pg=PA35&dq=Analyti

cal+Methods+for+Total+DOM+Pools&ots=J-9qcCUNUf&sig=Q944taPL98FVZYSAF6EBlCnkYtw&redir_esc=y#v=onepage&q=Analytical Methods for Total DOM Pools&f=false

Siegenthaler, U., & Sarmiento, J. L. (1993). Atmospheric carbon dioxide and the ocean. *Nature*, *365*(6442), 119–125. http://doi.org/10.1038/365119a0

Sijp, W. P., Gregory, J. M., Tailleux, R., & Spence, P. (2012). The Key Role of the Western Boundary in Linking the AMOC Strength to the North–South Pressure Gradient. *Journal of Physical Oceanography*, *42*(4), 628–643. http://doi.org/10.1175/JPO-D-11-0113.1

Sipler, R. E., & Bronk, D. A. (2015). *Biogeochemistry of Marine Dissolved Organic Matter*. *Biogeochemistry of Marine Dissolved Organic Matter*. http://doi.org/10.1016/B978-0-12-405940-5.00004-2

Skindersoe, M. E., Ettinger-epstein, P., Rasmussen, T. B., Bjarnsholt, T., Nys, R. De, & Givskov, M. (2008). Original Article Quorum Sensing Antagonism from Marine Organisms, *10*, 56–63. http://doi.org/10.1007/s10126-007-9036-y

Smith, R. C., & Baker, K. S. (1981). Optical properties of the clearest natural waters (200-800 nm). *Applied Optics*, *20*(2), 177–184. http://doi.org/10.1364/AO.20.000177

Stubbins, A., Niggemann, J., & Dittmar, T. (2012). Photo-lability of deep ocean dissolved black carbon. *Biogeosciences*, *9*(5), 1661–1670. http://doi.org/10.5194/bg-9-1661-2012

Sulzberger, B., & Durisch-Kaiser, E. (2009). Chemical characterization of dissolved organic matter (DOM): A prerequisite for understanding UV-induced changes of DOM absorption properties and bioavailability. *Aquatic Sciences*, *71*(2), 104–126. http://doi.org/10.1007/s00027-008-8082-5

Tedetti, M., & Sempéré, R. (2006). Penetration of ultraviolet radiation in the marine environment. A review. *Photochemistry and Photobiology*, *82*(2), 389–397. http://doi.org/10.1562/2005-11-09-lR-733

Weaver, A., Eby, M., & Wiebe, E. (2001). The UVic Earth System Climate Model: Model description, climatology, and applications to past, present and future climates. *Atmosphere- …*, *39*(4), 361–428. http://doi.org/10.1080/07055900.2001.9649686

Whitehead, R. F., De Mora, S. J., & Demers, S. (2000). Enhanced UV radiation—a new problem for the marine environment. *The Effects of UV Radiation in the Marine Environment*, 1–34. http://doi.org/10.1017/CBO9780511535444

Williams, P. M., & Druffel, E. R. M. (1987). Radiocarbon in dissolved organic matter in the central North Pacific Ocean. *Nature*, *330*, 246–248. http://doi.org/10.1038/330246a0

Yamanaka, Y., & Tajika, E. (1997). Role of dissolved organic matter in the marine biogeochemical cycle: Studies using an ocean biogeochemical general circulation model. *Global Biogeochemical Cycles*, *11*(4), 599–612. http://doi.org/10.1029/97GB02301

Yentsch, C. S., & Yentsch, C. M. (1982). The Attenuation of Light by Marine Phytoplankton with Specific Reference to the Absorption of Near-UV Radiation. In *The Role of Solar Ultraviolet Radiation in Marine Ecosystems* (pp. 691–700). Boston, MA: Springer US. http://doi.org/10.1007/978-1-4684-8133-4_60

# Declaration of Authorship

I, Jiajun WU, declare that this thesis and the work presented in it are my own and has been generated by me as the result of my own original research.

**Photochemical Degradation and the Global Cycling of Marine Biologically Refractory Dissolved Organic Matter Evaluated with the University of Victoria Earth System Climate Model**

I confirm that:

1. This work was done wholly or mainly while in candidature for a research degree at this University;
2. Where any part of this thesis has previously been submitted for a degree or any other qualification at this University or any other institution, this has been clearly stated;
3. Where I have consulted the published work of others, this is always clearly attributed;
4. Where I have quoted from the work of others, the source is always given. With the exception of such quotations, this thesis is entirely my own work;
5. I have acknowledged all main sources of help;

Signed:

Date: